DIGITALCOMMONS
—@WAYNESTATE—

Wayne State University

Wayne State University Dissertations

1-1-2017

Topics In High-Energy Physics: The Proton Magnetic Radius And Phenomenology Of Z0 Mediation Of Supersymmetry Breaking

Joydeep Roy
Wayne State University,

Follow this and additional works at: http://digitalcommons.wayne.edu/oa_dissertations

Part of the Physics Commons

Recommended Citation

TOPICS IN HIGH-ENERGY PHYSICS: THE PROTON MAGNETIC RADIUS AND PHENOMENOLOGY OF Z' MEDIATION OF SUPERSYMMETRY BREAKING

by

JOYDEEP ROY

DISSERTATION

Submitted to the Graduate School

of Wayne State University,

Detroit, Michigan

in partial fulfillment of the requirements

for the degree of

DOCTOR OF PHILOSOPHY

2017

MAJOR: PHYSICS

Approved By:

_____

Advisor   Date

_____

_____

_____

DEDICATION

To my dear father, Mr. Jitendra Nath Roy, without whose constant support I wouldn't have been here

ACKNOWLEDGMENTS

iv

LIST OF TABLES

LIST OF FIGURES

CHAPTER 1:   GENERAL INTRODUCTION

In this dissertation two topics in high-energy physics have been described. They both are quite interesting on their own merits. The 'Proton radius puzzle' which is elaborated later in this dissertation, has gained significant attention among the high-energy physics community in the last few years. Our first topic where the extraction of the magnetic radius of the proton is described is very closely related to that puzzle. The second topic of discussion is about supersymmetry and phenomenological discussion of the mediation of its breaking, combining anomaly and Z' mediation mechanisms. Imposition of the current LHC constraints on this mechanism is also described.

CHAPTER 2:   THE PROTON MAGNETIC RADIUS

2.1   Introduction

The proton is a fundamental constituent of matter. The first indication of the composite nature of the proton was the measurement of the magnetic moment of the proton by Frisch and Stern in 1933 [1]. The response of the proton to electromagnetic field is described by two form factors, one "electric" (G_E) and one "magnetic" (G_M). The magnetic moment of the proton is just the value of G_M at zero 4-momentum transfer squared. Viewed as a Taylor series, the magnetic moment is the first in an infinite list of numbers needed to describe the response of the proton to a magnetic field. The next number would be the slope of the magnetic form factor at zero, which is related to the magnetic radius of the proton. For the electric form factor, the value at zero is the total charge of the proton in units of e, and the slope at zero defines the charge radius of the proton. The electric and magnetic radii of the proton are therefore as fundamental as the charge and magnetic moment of the proton. Currently, we cannot determine them accurately from theory, although lattice QCD is making progress on this issue; see for example [2]. However they can be measured experimentally.

The determination of the charge radius of the proton has received considerable attention in the last few years as a result of the discrepancy between the extraction of the charge radius of the proton from muonic and regular hydrogen. The measurement reported by the CREMA collaboration in [3] has found $r_E^p = 0.84184(67)$ fm, and more recently [4] $r_E^p = 0.84087(39)$ fm. Both of these muonic hydrogen extractions are in conflict with the CODATA 2010 [5] value $r_E^p = 0.87580(770)$ fm, based on only hydrogen and deuterium spectroscopic data. This discrepancy is often referred to as the "proton radius puzzle."

The discrepancy has generated considerable debate. The discussion has focused on the

one hand on recalculation of the theoretical input to the extraction of r_E^p from muonic hydrogen and on modifications of the theoretical calculation such as proton structure effects and on effects of new physics, for references see [6].

Apart from regular and muonic hydrogen, electron proton scattering data also allows to measure the charge radius of the proton. Many such extractions exist in the literature, using different data sets and functional forms. The main problem in robust extraction of the proton charge radius from the data is the need to reliably extrapolate the form factor to $q^2 = 0$ in order to find its slope. Many of the existing extractions postulate a functional form for the form factor either explicitly, or implicitly by truncating a possibly general series expansion. Thus all of these extractions introduce model dependance for the value of r_E^p which is very hard to assess.

The problem was solved by Hill and Paz in [7], which introduced a method of extraction that is free of such model dependance. The method, often called the "z expansion" adapts an established tool in the study of *meson* form factors to the case of *baryon* form factors. The z expansion relies on the known analytic properties of the electromagnetic form factors G_E and G_M. They are analytic in the complex plane outside of a cut along the positive real q^2 axis that starts at $4m_\pi^2$ and extends to infinity. The location of the singularity also implies that the radius of convergence, if using a simple Taylor expansion for the form factors, is at most $4m_\pi^2$. Most of the data about the form factors is well above this value. But even if we use data that is strictly below it, it is questionable whether we can ignore higher terms in the Taylor expansion as it is often assumed. The z expansion avoids this difficulty. By using the variable z defined as

$$z(t, t_{\text{cut}}, t_0) = \frac{\sqrt{t_{\text{cut}} - t} - \sqrt{t_{\text{cut}} - t_0}}{\sqrt{t_{\text{cut}} - t} + \sqrt{t_{\text{cut}} - t_0}} \qquad (2.1.1)$$

we can map the domain of the analyticity of the form factors onto the unit circle; see Figure 2.2.1. For G_E and G_M, $t_{\text{cut}} = 4m_\pi^2$. The free parameter t_0 determines the location
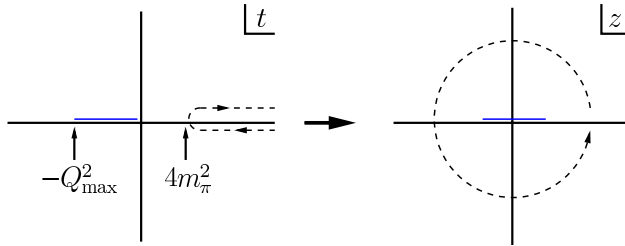
Figure 2.1.1: Conformal mapping of the cut plane to the unit circle.

of $z = 0$. Considered as a function of z, the form factor is analytic inside the unit circle and can be expressed as

$$G_{E,M}(q^2) = \sum_{k=0}^{\infty} a_k \, z(q^2)^k. \tag{2.1.2}$$

Intuitively, z is the "right" variable in which to perform a Taylor expansion of the form factor. Unlike a Taylor expansion in q^2, the expansion is guaranteed to converge for $|z| < 1$. Since for finite negative q^2, z is smaller than 1, this guarantees convergence for any q^2 measured in experiment. As an illustration to this intuitive picture, consider the proton magnetic form factor data tabulated in [8] and the neutron magnetic form factor data tabulated in [9, 10, 11, 12, 13, 14, 15]. Plotting the data points as a function of $Q^2 = -q^2$ for $0 < Q^2 \leq 1$ GeV^2, we see a considerable curvature; see Figure 2.1.2. If we plot the same data as a function of z (using $t_{\mathrm{cut}} = 4m_\pi^2$ and $t_0 = 0$) the data looks fairly linear. We can also easily estimate the slopes of the proton and neutron magnetic form factors. If we plot the normalized values of the form factors, i.e. the form factor values divided by their value at $q^2 = 0$ as a function of z, the slopes would be hard to distinguish. This implies that the magnetic radii of the proton and neutron are very similar. It will be shown later that this is indeed the case.

The magnetic radius of the proton is defined as $r_M^p \equiv \sqrt{\langle r^2 \rangle_M^p}$, where

$$\langle r^2 \rangle_M^p = \frac{6}{G_M^p(0)} \frac{d}{dq^2} G_M^p(q^2) \Big|_{q^2=0}. \tag{2.1.3}$$

In 2010 the A1 collaboration reported a value of $r_M^p = 0.777(13)_{\mathrm{stat.}}(9)_{\mathrm{syst.}}(5)_{\mathrm{model}}(2)_{\mathrm{group}}$
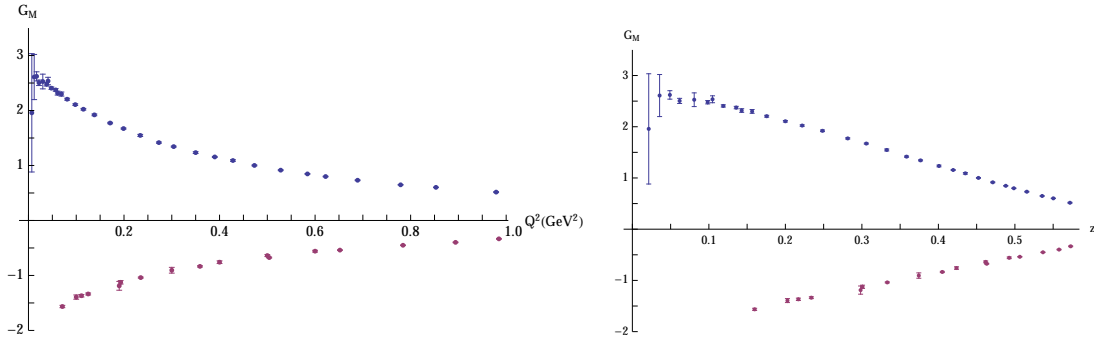
Figure 2.1.2: Proton (above the horizontal axes) and neutron (below the horizontal axes) magnetic form factor data as a function of Q^2 (left) and as a function of z (right). Here we choose $t_0 = 0$ and use $t_{\text{cut}} = 4m_\pi^2$ in the definition of z, and plot data for $0 \leq Q^2 \leq 1.0 \, \text{GeV}^2$.

fm [16]. This value is considerably lower than $r_M^p = 0.876 \pm 0.010 \pm 0.016$ fm extracted in [17] or 0.854 ± 0.005 fm extracted in [18], the two other extractions cited by the Particle Data Group (PDG) [19]. Is there also a *magnetic* radius puzzle?[1]

The purpose of this study is to apply the methods established in [7], to the extraction of the magnetic radius of the proton from scattering data. As in [7] we have utilized proton, neutron, and $\pi\pi$ scattering data to determine the magnetic radius of the proton from the reported measurement of the magnetic form factors of the proton and neutron. The magnetic radius of the neutron is also determined.

2.2   Form Factors and proton magnetic radius

The analytic structure of the form factors and their constraints were discussed in detail in [7]. Here we review some of the main ingredients needed for our analysis.

The Dirac and Pauli form factors, F_1^N and F_2^N, respectively, are defined as [20, 21]

$$\langle N(p')|J_\mu^{\text{em}}|N(p)\rangle = \bar{u}(p')\left[\gamma_\mu F_1^N(q^2) + \frac{i\sigma_{\mu\nu}}{2m_N}F_2^N(q^2)q^\nu\right]u(p), \qquad (2.2.1)$$

---

[1]See the conclusions for values of r_M^p not quoted by the PDG.

where $q^2 = (p' - p)^2 = t$ and N stands for p or n. The Sachs electric and magnetic form factors are related to the Dirac-Pauli basis by [22]

$$G_E^N(t) = F_1^N(t) + \frac{t}{4m_N^2} F_2^N(t), \quad G_M^N(t) = F_1^N(t) + F_2^N(t). \tag{2.2.2}$$

At $t = 0$ they are [19] $G_E^p(0) = 1$, $G_E^n(0) = 0$, $G_M^p(0) = \mu_p \approx 2.793$, $G_M^n(0) = \mu_n \approx -1.913$. We define the isoscalar and isovector form factors as

$$G_{M,E}^{(0)} = G_{M,E}^p + G_{M,E}^n, \quad G_{M,E}^{(1)} = G_{M,E}^p - G_{M,E}^n, \tag{2.2.3}$$

such that at $t = 0$ they are $G_E^{(0)}(0) = 1$, $G_E^{(1)}(0) = 1$, $G_M^{(0)}(0) = \mu_p + \mu_n$, $G_M^{(1)}(0) = \mu_p - \mu_n$. Here $G_{M,E}^p$ and $G_{M,E}^n$ stands for the proton and neutron form factors. Notice that $G_{M,E}^{(0)} = 2G_{M,E}^s$, $G_{M,E}^{(1)} = 2G_{M,E}^v$ for $G_{M,E}^{s,v}$ of [18].

2.2.1 Analyticity of form factors
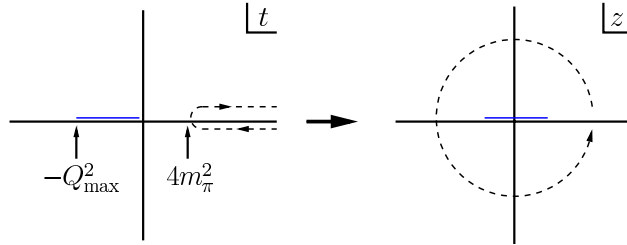
Figure 2.2.1: Conformal mapping of the cut plane to the unit circle.

The unknown functional behavior of the form factors makes it difficult to determine the number of parameters needed to fit experimental data. Therefore, the goal is to provide some constraints on the functional behavior of the form factors as shown in [7] by z-expansion method which is based upon the analytic properties of the form factor G_M^p. The z expansion relies on the known analytic properties of the electromagnetic form factors G_E and G_M. They are analytic functions of t outside of a cut that starts at the

two-pion threshold $t \geq 4m_\pi^2$ on the real t axis. The scattering data lies on $-Q_{\max}^2 \leq t \leq 0$, where $Q_{\max}^2$ denotes the largest value of Q^2 in a given data set. The domain of analyticity can be mapped onto the unit disk via the conformal transformation (2.1.1). The mapping is shown in Figure 2.2.1. The maximal value of $|z|$ depends on $Q_{\max}^2$ and t_0. It is minimized for the choice $t_0^{\mathrm{opt}} = t_{\mathrm{cut}} \left(1 - \sqrt{1 + Q_{\max}^2/t_{\mathrm{cut}}} \right)$ which is also the value used for Figure 2.2.1 .

Since the values of the form factors at $q^2 = 0$ are well known, in the following $t_0 = 0$ is used. As discussed in [7], the results do not depend on the choice of t_0. For this choice of t_0, the maximum value of $|z|$ is $0.46, 0.58$ for $Q_{\max}^2 = 0.5, 1.0$ GeV^2, respectively . The form factors can be expanded in a power series in $z(q^2)$:

$$G(q^2) = \sum_{k=0}^{\infty} a_k \, z(q^2)^k \, , \tag{2.2.4}$$

where higher order terms are suppressed by powers of the maximum values of $|z|$. The coefficients a_k are also bounded in size guaranteeing that the series converges.

The analytic structure in the t-plane, illustrated in the Fig.2.2.1 implies the dispersion relation,

$$G(t) = \frac{1}{\pi} \int_{t_{\mathrm{cut}}}^{\infty} dt' \, \frac{\mathrm{Im}G(t' + i0)}{t' - t} \, . \tag{2.2.5}$$

Parameterizing the unit circle by $z(t) = e^{i\theta}$ and solving eqn.2.2.4 for t with changed limits

we find [7]

$$a_0 = \frac{1}{\pi} \int_0^\pi d\theta \, \mathrm{Re} \, G[t(\theta) + i0] = G(t_0) \, ,$$

$$a_k = -\frac{2}{\pi} \int_0^\pi d\theta \, \mathrm{Im} \, G[t(\theta) + i0] \, \sin(k\theta)$$

$$= \frac{2}{\pi} \int_{t_{\mathrm{cut}}}^\infty \frac{dt}{t - t_0} \sqrt{\frac{t_{\mathrm{cut}} - t_0}{t - t_{\mathrm{cut}}}} \mathrm{Im} G(t) \sin[k\theta(t)] \, , \quad k \geq 1 \, , \qquad (2.2.6)$$

where

$$t = t_0 + \frac{2(t_{\mathrm{cut}} - t_0)}{1 - \cos\theta} \equiv t(\theta) \, . \qquad (2.2.7)$$

Knowledge of this imaginary part of $G(t)$ helps to put constraints on the coefficients a_k which is discussed in the next section.

2.2.2 Bounds on the coefficients

For a realistic extraction of the proton magnetic radius appropriate bounds on the coefficients a_k need to put. Hill and Paz [7] showed that in order to extract the electric charge radius r_E^p the bounds $|a_k| \leq 5, 10$ are conservative enough.

The vector dominance ansatz [6] was used to estimate the size of the a_k. Also from eqn. 2.2.3 the magnetic form factors at $q^2 = 0$ are given by $G_M^{(0)}(0) \approx 0.88$ and $G_M^{(1)}(0) \approx 4.7$, compared to $G_E^{(0,1)}(0) = 1$. Since the vector dominance ansatz is normalized by the value at $q^2 = 0$, coefficients are proportional to this value. Thus it is found that $|a_k| \leq 1.1$ for $I = 0$ and $|a_k| \leq 5.1$ for $I = 1$. Therefore it is concluded that $|a_k| \leq 5$ is too stringent and the looser bounds as $|a_k| \leq 10$ or $|a_k| \leq 15$ were used.

Since for the magnetic isovector form factor the singularities that are closest to the cut arise from the two pion continuum the imaginary part of $G_M^{(1)}$ close to the cut can be described by the pion form factor $F_\pi(t)$ (normalized to $F_\pi(0) = 1$) and $f_-^1(t)$, a partial

$\pi\pi \to N\bar{N}$ amplitude [18, 23, 24]:

$$\operatorname{Im} G_M^{(1)}(t) = \sqrt{\frac{2}{t}} \left(t/4 - m_\pi^2\right)^{\frac{3}{2}} F_\pi(t)^* f_-^1(t). \tag{2.2.8}$$

It is found that $a_0 \approx 7.9$, $a_1 \approx -5.5$, $a_2 \approx -6.1$, $a_3 \approx -2.9$, $a_4 \approx 1.1$ [6]. Also for the case of two nucleon threshold we used $e^+e^- \to N\bar{N}$ data to constrain the magnetic form factor. Calculations using these data showed that the contribution to $|a_k|$ in the region $t \geq 4m_N^2$ can be neglected [6].

One can also put a bound on the ratio $|\frac{a_k}{a_0}|$ which is explained in detail in [6]. Then from the known value of a_0 it is easy to put bounds on $|a_k|$. It was seen that the results from this bounds are consistent with the default bounds. Results are also independent of higher bound like $|a_k| \leq 20$.

Summary

All our studies point out that for the magnetic form factor the coefficients a_k are smaller than 10. Since $a_0 = G^{(1)}(0) = \mu_p - \mu_n \approx 4.7$, a bound of 5 might be too stringent. In the following the bounds of 10 and 15 were used instead of the bounds of 5 and 10 used in [7]. It will be seen that even using a bound of 20 will not change the results in an appreciable way.

One could also argue that a bound on the *ratio* $|a_k/a_0| \leq 5, 10$ is more appropriate. Since a_0 is known, this will translate to a bound of $|a_k| \leq 25, 50$ in the $I = 1$ case. It is preferable to use the more stringent bound of $|a_k| \leq 10, 15$, but comments on the results will be made while using these looser bounds.

It should be noted that for $t_0 = 0$, the magnetic radius depends only on the coefficient of z. Writing $G_M^p(q^2) = \sum_{k=0}^{\infty} a_k z(q^2)^k$, where $z(q^2) \equiv z(q^2, 4m_\pi^2, 0)$, equation (2.1.3) implies that

$$r_M^p = \frac{\hbar c}{2m_\pi c^2} \sqrt{-\frac{3a_1}{2\mu_p}}, \tag{2.2.9}$$

where the factors of $\hbar$ and c are explicitly shown. A bound of 5, 10, 15, or 20, on $|a_k|$, implies also a bound of 1.2, 1.6, 2.0, and 2.3 fm on r_M^p. Writing $G_M^{(0)}(q^2) = \sum_{k=0}^{\infty} a_k^{(0)} z(q^2, 9m_\pi^2, 0)^k$ and $G_M^{(1)}(q^2) = \sum_{k=0}^{\infty} a_k^{(1)} z(q^2, 4m_\pi^2, 0)^k$ we have

$$r_M^p = \frac{\hbar c}{2m_\pi c^2} \sqrt{-\frac{a_1^{(0)} + \frac{9}{4} a_1^{(1)}}{3\mu_p}}. \tag{2.2.10}$$

A bound of 5, 10, 15, or 20, on $|a_k^{(0,1)}|$, implies also a bound of 0.98, 1.4, 1.7, or 2.0 fm on r_M^p. For our default choice of bounds of 10 and 15 these values are much larger than the current range of values quoted by the PDG [19], roughly $0.7 - 0.9$ fm . Thus, just the presence of our default bounds does not bias the extraction of the radius.

2.3 Extraction of the proton magnetic radius

In this section the detail of the extraction of proton magnetic radius will be discussed.

2.3.1 Proton data

To extract the magnetic radius of proton the values of G_M^p from [8] were used. We write the form factor as $G_M^p(q^2) = \sum_{k=0}^{\infty} a_k z(q^2)^k$, where $z(q^2) \equiv z(q^2, 4m_\pi^2, 0)$. We fit $k < k_{max}$ parameters, where $k_{max} = 2, \ldots, 12$. We minimize the χ^2 function

$$\chi^2 = \sum_i (\text{data}_i - \text{theory}_i)^2 / (\sigma_i)^2, \tag{2.3.1}$$

where i ranges over the tabulated values of [8] up to a given maximal value of Q^2, with $Q^2 = 0.1, 0.2, \ldots, 1.2, 1.4, 1.6, 1.8$ GeV^2. As explained above, our default choice for the bounds on the coefficients is $|a_k| < 10$ and $|a_k| < 15$. The proton magnetic radius is obtained from (2.1.3). The error bars are determined from the $\Delta\chi^2 = 1$ range. Usually, the $\Delta\chi^2 = 1$ range was determined from a numerical search algorithm. For some higher

values of Q^2, the $\chi^2(r_M^p)$ seems to have some discontinuities and in that case, the $\Delta\chi^2 = 1$ was extracted directly from the $\chi^2(r_M^p)$ curve. To ensure a conservative estimate of the error, we quote only one digit in the error bar.

The extracted values and the value of the minimum of χ^2 do not vary with $k_{\max}$ for $k_{\max} > 4$. In other words, the extracted values do not depend on the number of coefficients we fit. In the following results with $k_{\max} = 8$ have been quoted. The extracted values of the magnetic radius are very consistent over the range of Q^2. Thus for data with $Q^2 \leq 0.5$ GeV^2, we have $r_M^p = 0.91^{+0.03}_{-0.06}$ fm for a bound of 10 and $r_M^p = 0.92^{+0.04}_{-0.07}$ fm for a bound of 15, while for $Q^2 \leq 1.0$ GeV^2 we have $r_M^p = 0.90^{+0.03}_{-0.07}$ fm for a bound of 10 and $r_M^p = 0.91^{+0.04}_{-0.07}$ fm for a bound of 15.

The dependence of the extracted magnetic radius on the bounds on $|a_k|$ have also been studied. If we use a bound of $|a_k| < 20$, the results above change to $r_M^p = 0.93^{+0.03}_{-0.07}$ fm for $Q^2 \leq 0.5$ GeV^2 and $r_M^p = 0.91^{+0.04}_{-0.08}$ fm for $Q^2 \leq 1.0$ GeV^2. These values are very similar to the ones obtained with $|a_k| < 10$ and $|a_k| < 15$. As discussed above the bound $|a_k| < 5$ is considered to be too stringent, but if it is used we obtained $r_M^p = 0.89^{+0.03}_{-0.05}$ fm for $Q^2 \leq 0.5$ GeV^2 and $r_M^p = 0.89^{+0.02}_{-0.05}$ fm for $Q^2 \leq 1.0$ GeV^2, which are not statistically different from the results of our default bounds.

Another possible choice of bounds might be to bound $|a_k/a_0|$. This is motivated by the fact that the vector dominance ansatz and the π-π data indicate that a_k/a_0 is similar for the electric and magnetic form factors. Thus we might choose $|a_k/a_0| < 5, 10$. We have checked the effect of these looser bounds on the extracted magnetic radius. For $Q^2 \leq 0.5$ GeV^2, we have $r_M^p = 0.92^{+0.03}_{-0.07}$ fm for a bound of $|a_k/a_0| < 5$ and $r_M^p = 0.95^{+0.04}_{-0.08}$ fm for a bound of $|a_k/a_0| < 10$ while for $Q^2 \leq 1.0$ GeV^2 we have $r_M^p = 0.91^{+0.04}_{-0.08}$ fm for a bound of $|a_k/a_0| < 5$ and $r_M^p = 0.92^{+0.05}_{-0.09}$ fm for a bound of $|a_k/a_0| < 10$. For the magnetic radius with $t_0 = 0$, $a_0 = \mu_p \approx 2.8$, so if $|a_k/a_0| < 5, 10$ were chosen, this translates to $|a_k| < 14, 28$ respectively. Comparing these results to the ones obtained above we notice a slight monotonic increase in the central value and the error bars with the loosening of

the bound. The increase in the error bars is to be expected of course. Even with the looser bounds, the results obtained are consistent with our default bounds.

Bound on a_k	r^p_M	$+\sigma$	$-\sigma$
5	0.89	0.03	0.05
10	0.91	0.03	0.06
15	0.92	0.04	0.07
20	0.93	0.04	0.07

Table 2.3.1: $Q^2 \leq 0.5$ GeV^2
Using proton data

Bound on a_k	r^p_M	$+\sigma$	$-\sigma$
5	0.89	0.02	0.05
10	0.91	0.03	0.07
15	0.91	0.04	0.07
20	0.91	0.05	0.08

Table 2.3.2: $Q^2 \leq 1.0$ GeV^2
Using proton data

Using our default bounds of $|a_k| < 10$ and $|a_k| < 15$, and using $Q^2 \leq 0.5$ GeV^2 for concreteness we obtain $r^p_M = 0.91^{+0.03}_{-0.06} \pm 0.02$ fm. The first error is for a bound of 10 and the second error includes the maximum variation of the $\Delta\chi^2 = 1$ interval when the fits are redone with a bound of 15. Some of the results are listed in Tables 2.3.1 and 2.3.2.

2.3.2 Proton and neutron data

Including neutron data allows us to separate the $I = 1$ and $I = 0$ isospin components of the proton magnetic form factor. Since for the $I = 0$ components $t_{\mathrm{cut}} = 9m^2_\pi$, this increases the value of t_{cut} and effectively decreases the maximum value of z.

As before values of G^p_M tabulated in [8] were used. For $G^n_M(Q^2)$ we used values published in [9, 10, 11, 12, 13, 14, 15][2]. The data reported in [26] and [27] were not used, as they were criticized for missing a systematic error, see section VIII of [14][3].

χ^2 was formed as before and G^n_M and G^p_M were expressed in terms of $G^{(0)}_M$ and $G^{(1)}_M$, see (2.2.3). We express $G^{(0)}_M$ as a power series in $z(t, 9m^2_\pi, 0)$ and $G^{(1)}_M$ as a power series

---

[2][14] contain the final results that supersedes the previous publications [28, 29]. For [15], the data is tabulated in [30].

[3]If we include these additional data points we obtain similar values of the magnetic radius but with much larger values of χ^2.

in $z(t, 4m_\pi^2, 0)$, i.e.

$$G_M^{(0)}(t) = \sum_k a_k^{(0)} z^k(t, t_{\text{cut}} = 9m_\pi^2, 0) \tag{2.3.2}$$

$$G_M^{(1)}(t) = \sum_k a_k^{(1)} z^k(t, t_{\text{cut}} = 4m_\pi^2, 0) \,. \tag{2.3.3}$$

As for the proton data alone, the extracted values of the magnetic radius do not depend on the number of the parameters we fit. The values are very consistent over the range of Q^2. Thus for data with $Q^2 \leq 0.5$ GeV^2, we have $r_M^p = 0.87_{-0.05}^{+0.04}$ fm for a bound of 10 and $r_M^p = 0.87_{-0.05}^{+0.05}$ fm for a bound of 15, while for $Q^2 \leq 1.0$ GeV^2 we have $r_M^p = 0.87_{-0.05}^{+0.03}$ fm for a bound of 10 and $r_M^p = 0.88_{-0.05}^{+0.04}$ fm for a bound of 15. These values are consistent with the values extracted from the proton data alone.

The dependence of the extracted magnetic radius on the bounds on $|a_k|$ were studied. If a bound of $|a_k| < 20$ is used, the results above change to $r_M^p = 0.88_{-0.06}^{+0.04}$ fm for $Q^2 \leq 0.5$ GeV^2 and $r_M^p = 0.88_{-0.06}^{+0.05}$ fm for $Q^2 \leq 1.0$ GeV^2. These values are very similar to the ones obtained with $|a_k| < 10$ and $|a_k| < 15$. On the other hand if the bound $|a_k| < 5$ is used, we obtain $r_M^p = 0.87_{-0.02}^{+0.02}$ fm for $Q^2 \leq 0.5$ GeV^2 and $r_M^p = 0.87_{-0.02}^{+0.02}$ fm for $Q^2 \leq 1.0$ GeV^2. The central values are consistent with our default bounds, but the error bars are substantially smaller. This is to be expected since this bound is too stringent.

As explained above, another possible choice of bounds is $|a_k/a_0| < 5, 10$. For $Q^2 \leq 0.5$ GeV^2, we have in this case $r_M^p = 0.88_{-0.06}^{+0.05}$ fm for a bound of $|a_k/a_0| < 5$ and $r_M^p = 0.91_{-0.07}^{+0.05}$ fm for a bound of $|a_k/a_0| < 10$. For $Q^2 \leq 1.0$ GeV^2 we have $r_M^p = 0.89_{-0.07}^{+0.04}$ fm for a bound of $|a_k/a_0| < 5$ and $r_M^p = 0.90_{-0.09}^{+0.05}$ fm for a bound of $|a_k/a_0| < 10$. Since $a_0^{(0)} = \mu_p + \mu_n \approx 0.88$, $a_0^{(1)} = \mu_p - \mu_n \approx 4.7$, $|a_k^{(0)}/a_0^{(0)}| < 5$ implies $|a_k^{(0)}| < 4.4$ and $|a_k^{(1)}/a_0^{(1)}| < 5$ implies $|a_k^{(1)}| < 23.5$. Similarly $|a_k^{(0)}/a_0^{(0)}| < 10$ implies $|a_k^{(0)}| < 8.8$ and $|a_k^{(1)}/a_0^{(1)}| < 10$ implies $|a_k^{(1)}| < 47$. Comparing these results to the ones obtained above we notice again a monotonic increase in the central value and the error bars with the loosening of the bound. The increase in the error bars is to be expected of course. Even

with the looser bounds, the results obtained are consistent.

Bound on a_k	r_M^p	$+\sigma$	$-\sigma$
5	0.86	0.02	0.01
10	0.87	0.04	0.05
15	0.87	0.05	0.05
20	0.88	0.04	0.06

Table 2.3.3: $Q^2 \leq 0.5$ GeV^2 Using proton and neutron data

Bound on a_k	r_M^p	$+\sigma$	$-\sigma$
5	0.87	0.02	0.02
10	0.88	0.02	0.05
15	0.88	0.04	0.05
20	0.88	0.05	0.06

Table 2.3.4: $Q^2 \leq 1.0$ GeV^2 Using proton and neutron data

Using our default bounds of $|a_k| < 10$ and $|a_k| < 15$, and using $Q^2 \leq 0.5$ GeV^2 for concreteness we obtain $r_M^p = 0.87^{+0.04}_{-0.05} \pm 0.01$ fm. The results are shown in Tables 2.3.3 and 2.3.4.

2.3.3 Proton, neutron and $\pi\pi$ data

Between the two-pion and four-pion threshold the only state that can contribute to the imaginary part of the magnetic isovector form factor is that of two pions. Since the information about $\mathrm{Im}\,G_M^{(1)}(t)$ in this region is known to us, see (2.2.8), we can use it to raise the effective threshold for the isovector form factor from $t_{\mathrm{cut}} = 4m_\pi^2$ to $t_{\mathrm{cut}} = 16m_\pi^2$. It is done by fitting [7]

$$G_M^{(1)}(t) = G_{\mathrm{cut}}(t) + \sum_k a_k^{(1)} z^k(t, t_{\mathrm{cut}} = 16m_\pi^2, 0). \tag{2.3.4}$$

$G_{\mathrm{cut}}(t)$ is calculated using (2.2.5) from the discrete expression for $\mathrm{Im}\,G_M^{(1)}(t)$ described in section 2.2.2. As in [7] two cases for $G_{\mathrm{cut}}(t)$ were considered. The first is generated by the values of $\mathrm{Im}\,G_M^{(1)}(t)$ in the range $4m_\pi^2 < t < 16m_\pi^2$, and the second by the values of $\mathrm{Im}\,G_M^{(1)}(t)$ in the range $4m_\pi^2 < t < 40m_\pi^2$. The second choice amounts to modeling the $\pi\pi$ continuum $16m_\pi^2 < t < 40m_\pi^2$ by $\mathrm{Im}\,G_M^{(1)}(t)$ of (2.2.8). As explained in [7], this does not introduce model dependence since the difference between the true continuum and $G_{\mathrm{cut}}(t)$ will be accounted for by the parameters in the z expansion, as the value of $t_{\mathrm{cut}} = 16m_\pi^2$

is not changed.

In [7] it was found that the second choice of $G_{\mathrm{cut}}(t)$ led to a smaller size of the coefficients in the z expansion of the isovector form factor. It will be interesting to check if that holds true also in the magnetic case. We fit the same proton and neutron data for $Q^2_{\max} = 1$ GeV^2, $t_0 = 0$, $k_{\max} = 8$ and a bound of 15 on the coefficients using (2.3.4). For the first choice of $G_{\mathrm{cut}}(t)$ we find the first two coefficients of the isoscalar form factor to be $-2^{+0.5}_{-0.3}, 3^{+2}_{-6}$ and the first two coefficients of the vector form factor to be $-13.5(3), 13^{+6}_{-3}$ (the value of 13^{+6}_{-3} was obtained by applying a bound of 15 on all the coefficients with the exception of the second one, which is left unbounded). For the second choice of $G_{\mathrm{cut}}(t)$ it is found that the first two coefficients of the isoscalar form factor are not changed while the first two coefficients of the vector form factor are $2.6^{+0.4}_{-0.5}, 5^{+5}_{-4}$. As in the electric form factor case, there is a reduction in the size of the isovector coefficients when using the second form. We will therefore adopt that as our default choice. As it will be shown below, the value of the magnetic radius does not change if the first form of $G_{\mathrm{cut}}(t)$ is used.

We can understand the large size of the isovector coefficients when using $G_{\mathrm{cut}}(t)$ calculated from $\mathrm{Im}\, G_M^{(1)}(t)$ in the range $4m_\pi^2 < t < 16m_\pi^2$. From equations (2.2.3) and (2.3.4), the proton magnetic radius is given by

$$r^p_M = \frac{\hbar c}{2m_\pi c^2} \sqrt{\frac{1}{\mu_p}\left(-\frac{1}{3}a_1^{(0)} - \frac{3}{16}a_1^{(1)} + 4m_\pi^2 c^4 G'_{\mathrm{cut}}(0)\right)}, \qquad (2.3.5)$$

where $G'_{\mathrm{cut}}(0)$ is obtained from (2.2.5)

$$G'_{\mathrm{cut}}(0) = \frac{1}{\pi}\int_{4m_\pi^2} dt' \frac{\mathrm{Im}G(t' + i0)}{(t')^2}. \qquad (2.3.6)$$

Since $\mathrm{Im}\, G_M^{(1)}(t)$ from (2.2.8) is positive in the relevant region, as the upper limit in (2.3.6) is increased, $G'_{\mathrm{cut}}(0)$ increases. Therefore $G'_{\mathrm{cut}}(0)$ calculated from $\mathrm{Im}\, G_M^{(1)}(t)$ in the

range $4m_\pi^2 < t < 16m_\pi^2$ is smaller than $G'_{\text{cut}}(0)$ calculated from $\text{Im}\, G_M^{(1)}(t)$ in the range $4m_\pi^2 < t < 40m_\pi^2$ and as a result $|a_1^{(1)}|$ must be larger to maintain the same size of r_M^p preferred by the data. In fact, since we can calculate $G'_{\text{cut}}(0)$, if we *assume* $r_M^p \approx 0.87$ fm and use $a_1^{(0)} \approx -2$, we can calculate and find $a_1^{(1)} \approx -13$ in the first case and $a_1^{(1)} \approx 3$ in the second case. These are the values we obtained above

Using (2.3.4) the magnetic radius was extracted. The extracted values of the magnetic radius do not depend on the number of the parameters we fit. The values are very consistent over the range of Q^2. Thus for data with $Q^2 \leq 0.5$ GeV^2, we have $r_M^p = 0.871_{-0.015}^{+0.011}$ fm for a bound of 10 and $r_M^p = 0.873_{-0.016}^{+0.012}$ fm for a bound of 15, while for $Q^2 \leq 1.0$ GeV^2 we have $r_M^p = 0.874_{-0.015}^{+0.008}$ fm for a bound of 10 and $r_M^p = 0.874_{-0.014}^{+0.012}$ fm for a bound of 15. These values are consistent with the values extracted above.

We have studied the dependence of the radius on the bounds on the coefficients. If a bound of 20 is used, $r_M^p = 0.876_{-0.018}^{+0.012}$ for $Q^2 \leq 0.5$ GeV^2 and $r_M^p = 0.875_{-0.016}^{+0.013}$ for $Q^2 \leq 1.0$ GeV^2. These values are very similar to the ones obtained with a bound of 10 and 15. If we use the too-stringent bound of 5 we obtain $r_M^p = 0.867_{-0.013}^{+0.010}$ for $Q^2 \leq 0.5$ GeV^2 and $r_M^p = 0.867_{-0.008}^{+0.006}$ for $Q^2 \leq 1.0$ GeV^2. These values are consistent, but the error bars are smaller.

Another possible choice of bounds is $|a_k/a_0| < 5, 10$. For $Q^2 \leq 0.5$ GeV^2, we find $r_M^p = 0.867_{-0.013}^{+0.013}$ fm for a bound of $|a_k/a_0| < 5$ and $r_M^p = 0.869_{-0.015}^{+0.013}$ fm for a bound of $|a_k/a_0| < 10$. For $Q^2 \leq 1.0$ GeV^2, we find $r_M^p = 0.867_{-0.009}^{+0.008}$ fm for a bound of $|a_k/a_0| < 5$ and $r_M^p = 0.873_{-0.014}^{+0.009}$ fm for a bound of $|a_k/a_0| < 10$. All these results are consistent with our default choices.

The decrease in the error bars when including the $\pi\pi$ data arises from the increase in the value of t_{cut} from $4m_\pi^2$ to $16m_\pi^2$ for the isovector form factor. If we use (2.3.4) but with $t_{\text{cut}} = 4m_\pi^2$ we obtain results that are almost identical to the fits using the proton and neutron data alone. As another check of our results, we fit the data using (2.3.4), but with $G_{\text{cut}}(t)$ calculated using $\text{Im}\, G_M^{(1)}(t)$ in the range $4m_\pi^2 < t < 16m_\pi^2$. As

discussed above, we use only a bound of 15 in this case. For $Q^2 \leq 0.5$ GeV^2 we find $r_M^p = 0.873^{+0.011}_{-0.016}$, and for $Q^2 \leq 1.0$ GeV^2 we find $r_M^p = 0.873^{+0.012}_{-0.012}$. These values are very close to the ones we obtained with the use of the default form of $G_{\mathrm{cut}}(t)$.

The expression for Im $G_M^{(1)}(t)$ depends on $f_-^1(t)$. The tabulation of $f_-^1(t)$ in [25] does not quote any error. In [7] an error of 30% was used as a representative uncertainty. If we assume a 30% increase for $f_-^1(t)$ and hence for $G_{\mathrm{cut}}(t)$ we obtain for $Q^2 \leq 0.5$ GeV^2 and a bound of 10, $r_M^p = 0.872^{+0.013}_{-0.015}$. If we assume a 30% decrease for $G_{\mathrm{cut}}(t)$ we obtain for $Q^2 \leq 0.5$ GeV^2 and a bound of 10, $r_M^p = 0.867^{+0.010}_{-0.015}$.

Bound on a_k	r_M^p	$+\sigma$	$-\sigma$
5	0.867	0.010	0.013
10	0.871	0.011	0.015
15	0.873	0.012	0.016
20	0.876	0.012	0.018

Table 2.3.5: $Q^2 \leq 0.5$ GeV^2 Using proton, neutron and $\pi\pi$ data

Bound on a_k	r_M^p	$+\sigma$	$-\sigma$
5	0.867	0.006	0.008
10	0.874	0.008	0.015
15	0.874	0.012	0.014
20	0.875	0.013	0.016

Table 2.3.6: $Q^2 \leq 1.0$ GeV^2 Using proton, neutron and $\pi\pi$ data

In summary, all our checks produce consistent results for r_M^p. Using our default choices for the bounds and $G_{\mathrm{cut}}(t)$, and using $Q^2 \leq 0.5$ GeV^2 for concreteness we obtain $r_M^p = 0.87^{+0.02}_{-0.02}$ fm. Our conservative error estimate includes the variation of the bounds and of $G_{\mathrm{cut}}(t)$ where we choose to quote only one digit in our error estimate. The results are summarized in Tables 2.3.5 and 2.3.6.

2.4 Extraction of the neutron magnetic radius

The data used to extract the magnetic radius of the proton can be used also to extract the magnetic radius of the neutron. The magnetic radius of the neutron is defined as $r_M^n \equiv \sqrt{\langle r^2 \rangle_M^n}$, where

$$\langle r^2 \rangle_M^n = \frac{6}{G_M^n(0)} \frac{d}{dq^2} G_M^n(q^2) \bigg|_{q^2=0}. \tag{2.4.1}$$

We extract the neutron magnetic radius from the neutron, neutron and proton, and neutron, proton, and $\pi\pi$ data sets. We follow the same default choices described above. In particular we will use a bound of 10 and 15 on the coefficients of the z expansion.

2.4.1 Neutron data

Using the neutron form factor data reported in [9, 10, 11, 12, 13, 14, 15] we fit $G_M^n(q^2) = \sum_{k=0}^{\infty} a_k \, z(q^2)^k$ by minimizing the χ^2 function of (2.3.1). For a cut $Q^2 \leq 0.5$ GeV^2 we find $r_M^n = 0.74^{+0.13}_{-0.06}$ fm for a bound of 10 and $r_M^n = 0.65^{+0.21}_{-0.07}$ fm for a bound of 15. For a cut of $Q^2 \leq 1.0$ GeV^2 we find $r_M^n = 0.77^{+0.17}_{-0.09}$ fm for a bound of 10 and $r_M^n = 0.74^{+0.20}_{-0.11}$ fm for a bound of 15. Obviously the error bars for r_M^n extracted from the neutron data are much larger than for r_M^p. We prefer to quote only one digit in our error bar. We therefore determine $r_M^n = 0.7^{+0.2}_{-0.1}$ fm from neutron data alone. Comparing to $r_M^p = 0.91^{+0.03}_{-0.06} \pm 0.02$ fm obtained from proton data alone, we find that r_M^n and r_M^p are consistent within errors.

2.4.2 Neutron and proton data

Adding the proton form factor data from [8] allows us to separate the isospin components. The magnetic radius of the neutron is given by an equation similar to (2.2.10)

$$r_M^n = \frac{\hbar c}{2 m_\pi c^2} \sqrt{\frac{-a_1^{(0)} + \frac{9}{4} a_1^{(1)}}{3 \mu_n}}. \tag{2.4.2}$$

We fit the isoscalar and the isovector form factors as described before. For a cut $Q^2 \leq 0.5$ GeV^2 we find $r_M^n = 0.89^{+0.06}_{-0.09}$ fm for a bound of 10 and $r_M^n = 0.88^{+0.08}_{-0.09}$ fm for a bound of 15. For a cut of $Q^2 \leq 1.0$ GeV^2 we find $r_M^n = 0.88^{+0.06}_{-0.08}$ fm for a bound of 10 and $r_M^n = 0.89^{+0.07}_{-0.10}$ fm for a bound of 15. Again the error bars for r_M^n are about twice as large as those for r_M^p from the same data set. Quoting only one digit we determine $r_M^n = 0.9^{+0.1}_{-0.1}$

fm from neutron and proton data. Comparing to $r_M^p = 0.87^{+0.04}_{-0.05} \pm 0.02$ fm obtained from the same proton and neutron data, we find that r_M^n and r_M^p are consistent within errors.

2.4.3 Neutron, proton, and $\pi\pi$ data

Adding the $\pi\pi$ data as described in the previous section leads to a reduction in the error bars. For a cut $Q^2 \leq 0.5$ GeV^2 we find $r_M^n = 0.89^{+0.03}_{-0.03}$ fm for a bound of 10 and $r_M^n = 0.89^{+0.03}_{-0.03}$ fm for a bound of 15. If we take a 30% variation of $f_-^1(t)$ as described above, we get values of r_M^n within this range. For a cut of $Q^2 \leq 1.0$ GeV^2 we find $r_M^n = 0.88^{+0.03}_{-0.01}$ fm for a bound of 10 and $r_M^n = 0.88^{+0.03}_{-0.02}$ fm for a bound of 15. As before the error bars for r_M^n are about twice as large as those for r_M^p from the same data set. Quoting only one digit for the error bars we determine $r_M^n = 0.89^{+0.03}_{-0.03}$ fm from neutron, proton, and $\pi\pi$ data. Comparing to $r_M^p = 0.87^{+0.02}_{-0.02}$ fm obtained from the same data set, we find that r_M^n and r_M^p are consistent within errors.

Neutron magnetic radius results are summarized in Table 2.4.1.

Q^2(GeV^2)	Bound on a_k	Neutron data			Neutron and Proton data			Neutron,Proton and $\pi\pi$ data		
		r_M^n	$+\sigma$	$-\sigma$	r_M^n	$+\sigma$	$-\sigma$	r_M^n	$+\sigma$	$-\sigma$
	10	0.74	0.13	0.06	0.89	0.06	0.09	0.89	0.03	0.03
0.5	15	0.65	0.21	0.07	0.88	0.08	0.09	0.89	0.03	0.03
1.0	10	0.77	0.17	0.09	0.88	0.06	0.08	0.88	0.03	0.01
	15	0.74	0.20	0.11	0.89	0.07	0.10	0.88	0.03	0.02

Table 2.4.1: Neutron magnetic radii for different data sets

2.5 Conclusion

The purpose of this analysis was to try to resolve the discrepancies that exist in the literature regarding the extraction of the magnetic radius of the proton. To achieve that we used the "z-expansion" method which incorporates the analytic structure of the form factors.

Three data sets have been used for the extraction. From the proton data set we extracted the magnetic radius of the proton as $r_M^p = 0.91^{+0.03}_{-0.06} \pm 0.02$ fm. Inclusion of the neutron data gives the radius $r_M^p = 0.87^{+0.04}_{-0.05} \pm 0.01$ fm. When we add the $\pi\pi$ data along with these data sets the extracted value of the magnetic radius is $r_M^p = 0.87^{+0.02}_{-0.02}$ fm. Our study has also revealed that the extracted magnetic radius is independent of the number of parameters we fit or the range of Q^2 we used. We have reported all our results with 8 parameters and two specific ranges of energy $Q^2 \leq 0.5$ GeV^2 and $Q^2 \leq 1.0$ GeV^2.

The same procedure was applied to extract the magnetic radius of the neutron. Combining all three data sets (neutron, proton and $\pi\pi$) we extract the radius of the neutron to be $r_M^n = 0.89 \pm 0.03$ fm. Interestingly we notice that within the errors this value is consistent with the magnetic radius of the proton $r_M^p = 0.87 \pm 0.02$ fm.

Recently Particle Data Group (PDG) [31] has listed both of these values $r_M^p = 0.87 \pm 0.02$ fm and $r_M^n = 0.89 \pm 0.03$ fm in their listing of magnetic radius of proton and neutron respectively.

CHAPTER 3: IMPOSING LHC CONSTRAINTS ON THE COMBINED ANOMALY AND Z' MEDIATION MECHANISM OF SUPERSYMMETRY BREAKING

3.1   Introduction

All fundamental particles that known to exist in nature can be categorized as either fermions or bosons. Supersymmetry (SUSY) is a symmetry that is assumed to exist between the fermions and the bosons. One of the prime success of supersymmetric theory is to stabilize the Higgs mass and solve the hierarchy problem. The absence of 'superpartner' of the electron, 'selectron' and other experimental facts (to be discussed later) have revealed that supersymmetry must be a broken symmetry. Detailed study of different supersymmetry breaking scenarios indicate that our known particle and energy sectors need to be extended to accommodate the SUSY breaking effects. Therefore it is believed that SUSY is broken presumably at very high energy level, known as 'hidden sector' and then these breaking effects are 'communicated' to the Electroweak (EW) scale, known as 'visible sector'. Therefore the most important questions in supersymmetric theory are, 'how the sypersymmetry is broken and how this breakdown is communicated between the two sectors' ? There are several supersymmetry breaking mechanisms available in the literature, like gauge-mediated-supersymmetry-breaking (GMSB), Planck-mediated-supersymmetry-breaking (PMSB), Anomaly mediation etc. For our purpose we consider the anomaly mediation and Z' mediation mechanisms. Combining anomaly with Z' mediation allows us to solve the tachyonic problem of the former and avoid fine tuning in the latter. This model includes an extra $U(1)'$ gauge symmetry and extra singlet scalar S which provides a solution to the 'μ problem' of the Minimal Supersymmetric Standard Model (MSSM). The low-energy particle spectrum is calculated from the Renormalization Group Equations (RGEs'). The benchmark points considered in the original model,

suggested before the Higgs discovery, predicted a Higgs mass heavier than the generic MSSM value. In 2012, the Higgs particle was discovered and found to have a mass of 125 GeV. Therefore, we can use that value and other current Large Hadron Collider (LHC) data to scan the parameter space and update the predictions of the model, in particular the mass of the Z' gauge boson.

3.2 Some basics of Supersymmetry

In this section we briefly discuss the motivations that lead to the concept of super-symmetry and how to build up a supersymmetric Lagrangian.

3.2.1 Motivation of Supersymmetry

The Standard Model (SM) of high-energy physics is experimentally proven to describe many physical phenomena with significant level of accuracy. Still there are several issues at high-energy physics that need to be addressed and that requires physics beyond the Standard Model. We will discuss few of them as the prime motivation for the introduction of the concept of supersymmetry.

Quadratic divergences in SM

When we study the quantum field theory to understand the physics of fundamental particles we are interested in the invariant matrix element $\mathcal{M}$ which is defined as [32]

$$\langle \mathbf{p_1 p_2} \dots |iT| \mathbf{k}_\mathcal{A} \mathbf{k}_\mathcal{B} \rangle = (2\pi)^4 \delta^{(4)}(k_\mathcal{A} + k_\mathcal{B} - \sum p_f) \cdot i\mathcal{M}(k_\mathcal{A}, k_\mathcal{B} \to p_f). \qquad (3.2.1)$$

where $\mathcal{A}, \mathcal{B}$ are the incoming particles with 4-momentum $k_\mathcal{A}, k_\mathcal{B}$ respectively. After the collision they are producing n no of particles with 4-momenta p_1, p_2 etc. T is the matrix which contain all the informations regarding the interactions between the colliding

particles.

What $\mathcal{M}$ basically calculates is the transition amplitudes which are determined by the contribution of all possible Feynman diagrams for the process under consideration. Calculation of tree-level Feynman diagrams are straight-forward once we determine the Feynman rules for the vertex and propagators from the Lagrangian describing the process. The complications arises when the loop-diagrams consisting of virtual particles are considered.
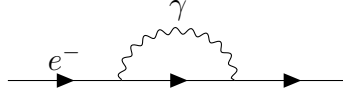
Figure 3.2.1: Electron self-energy diagram

For example, let us first consider the electron self-energy correction shown in the Figure 3.2.1. The two-point function of this 1-loop diagram is given by

$$
\begin{aligned}
\sum(k) &= \int \frac{d^4k}{(2\pi)^4} \left[(-ie\gamma^\mu) \frac{i}{\not{k}-m_0}(-ie\gamma^\nu)\left(\frac{-ig_{\mu\nu}}{k^2}\right) \right] \\
&= -e^2 \int \frac{d^4k}{(2\pi)^4} \left[\frac{\gamma^\mu\gamma^\nu g_{\mu\nu}}{(\not{k}-m_0)k^2} \right] \\
&= -e^2 \int \frac{d^4k}{(2\pi)^4} \left[\frac{\gamma^\mu(\not{k}+m_0)\gamma_\mu}{(k^2-m_0^2)k^2} \right] \\
&= -e^2 \int \frac{d^4k}{(2\pi)^4} \left[\frac{-2\not{k}}{(k^2-m_0^2)k^2} + \frac{4m_0}{(k^2-m_0^2)k^2} \right],
\end{aligned}
$$

$$(3.2.2)$$

where m_0 is the 'bare' electron mass obtained from the pole of the electron propagator. Clearly we find that the second term of eqn. 3.2.2 gives a finite contribution, but the first term gives a contribution to the bare mass which varies with the cut-off momentum Λ as

$$
\delta m \sim \alpha \int^\Lambda \frac{d^4k}{\not{k}k^2} \tag{3.2.3}
$$
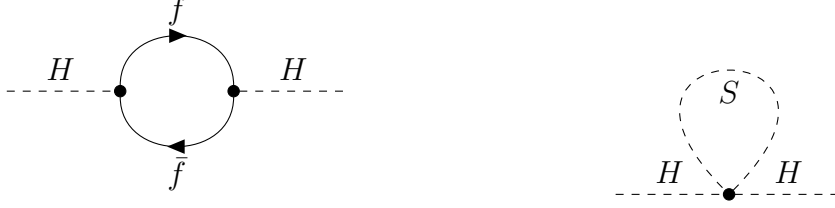
Figure 3.2.2: Higgs self-energy due to a fermion f

Figure 3.2.3: Higgs self-energy due to a scalar S

with $\alpha = \frac{g^2}{4\pi}$, g being the $U(1)$ coupling constant. Final calculation shows that the exact correction is of the amount

$$\delta m = \frac{3\alpha}{4\pi} m_0 \log(\frac{\Lambda^2}{m_0^2}). \tag{3.2.4}$$

The presence of the logarithm in eqn.3.2.4 ensures that even if Λ is of the order of Plank scale, $M_{\text{Pl}}(= [8\pi G_{\text{Newton}}]^{-1/2} = 2.4 \times 10^{18}$ GeV), the change in mass is proportional to m_0 and we get the 'physical' mass of the electron as $m_e = m_0 + \delta m$. If $m_0 = 0$, the quantum correction is also 0, following eqn. 3.2.4. Everything seems nice and under control.

Now let us focus on the 1-loop diagram of scalar fields as shown in Figure 3.2.2 where a fermion (f) is emitted and again reabsorbed during the propagation of a Higgs field (H). The two-point function in this case is given by

$$\begin{aligned}
\sum(k) &= -\int \frac{d^4k}{(2\pi)^4} \text{tr}\left[(i\frac{\lambda_f}{\sqrt{2}})\frac{i(\not{k}+m_f)}{k^2-m_f^2}(i\frac{\lambda_f}{\sqrt{2}})\frac{i(\not{k}+m_f)}{k^2-m_f^2}\right] \\
&= -N(f)\lambda_f^2 \int \frac{d^4k}{(2\pi)^4}\left[\frac{k^2+m_f^2}{(k^2-m_f^2)^2}\right] \\
&= -N(f)\lambda_f^2 \int \frac{d^4k}{(2\pi)^4}\left[\frac{1}{(k^2-m_f^2)} + \frac{2m_f^2}{(k^2-m_f^2)^2}\right],
\end{aligned}$$

$$\tag{3.2.5}$$

where $N(f)$ is a multiplicity factor, 3 for top quark and so on.

Similar as electron self-energy case, the second term of eqn. 3.2.5 gives a finite con-

tribution ($\int \frac{d^4k}{k^4}$). Whereas for $k >> m_f$, the first term is quadratically divergent and therefore the correction ($\Lambda^2 \sim M_{\text{Pl}}^2$) is almost 30 orders magnitude larger than the Higgs mass.

Comparing and analyzing two cases of radiative corrections for the electron and for Higgs particle, we find an important aspect of the SM Lagrangian, *symmetry*. In the Quantum Electrodynamical (QED) part of SM Lagrangian, there exist a symmetry known as *chiral symmetry*. In the limit of this symmetry ($m \to 0$) a fermion mass does not receive any radiative correction and a perfect symmetry exists. Since electron is not massless, this quantity (m_0) is breaking this symmetry. Therefore those corrections must be proportional to their bare masses only and also depend on the cut-off scale logarithmically. Thus it is said that chiral symmetry 'protects' the fermion masses from the loop corrections. In the case of scalars there is no such symmetry which is equivalent to the chiral symmetry for fermions that protects them from acquiring large radiative corrections. Therefore there is a need to introduce some new kind of symmetry which can address this problem.

Hierarchy problem

The discussion of the 'hierarchy problem' starts with the two fundamental energy scales of nature that seem to exist till now, namely electroweak scale ($m_{\text{EW}} \sim 10^3$ GeV) and the Planck scale ($M_{\text{Pl}} \sim 10^{18}$ GeV). Why do we care so much about these two scales only ? The reason is that the first one is relevant because most of our observed fundamental or composite particles are found at or below this scale. Whereas at the Planck scale the gravitational force become significantly strong. The enormous difference between these two scale (which is in simplest term known as the 'hierarchy problem') is definitely a matter of concern and the issue has rightfully taken many particle physicist's good amount of lifetime!

Hierarchy problem is also very much related to the divergences described above and

the renormalization procedure. As we have seen above, when the Higgs particle couple to a fermion with mass close to the cut-off scale, eqn. 3.2.5 tells us that the divergent contribution would be enormous [33],

$$\Delta m_H^2 \sim -\frac{|\lambda_f|^2}{8\pi^2}\Lambda_{\text{UV}}^2 + \ldots \tag{3.2.6}$$

and consequently a large amount of fine-tuning would be needed.

The Higgs particle can also receive huge quantum corrections from heavy scalars S (Figure 3.2.3) or other particles which can directly or indirectly couple to it as explained in [33]

$$\Delta m_H^2 \sim \frac{\lambda_S}{16\pi^2}\left[\Lambda_{\text{UV}}^2 - \ldots\right]. \tag{3.2.7}$$

Now let us consider the classical Higgs potential

$$V = -\mu^2\phi^\dagger\phi + \frac{\lambda}{4}(\phi^\dagger\phi)^2 \tag{3.2.8}$$

where μ is the Higgs mass parameter, ϕ is a $SU(2)$ doublet field

$$\phi = \begin{pmatrix} \phi^+ \\ \phi^0 \end{pmatrix} \tag{3.2.9}$$

and λ is the strength of Higgs self-coupling. Clearly the minimum of the Higgs potential gives the relation $\lambda|\phi|^2 = 2\mu^2$ leads to

$$|\phi| = \mu\sqrt{\frac{2}{\lambda}} \equiv \frac{v}{\sqrt{2}} \tag{3.2.10}$$

where v is known as the *vacuum expectation value* (vev), determined from the minimum of the classical potential 3.2.8. Experimental measurements of the properties of electroweak

interactions tells us the value of v to be 246 GeV. This is the electroweak scale mentioned earlier and determines all the masses of the theory at the tree-level.

A very obvious and fundamental question then arises, if there exists a more fundamental theory than the SM at higher energy (may be at M_{Pl} scale) then why the mass-squared parameter μ^2 is 15 order magnitude less ? One way to solve this problem is to think about a procedure which can prevent the μ^2 term from acquiring such large contribution and then we don't need to worry about the difference between these fundamental energy scales. The concept of supersymmetry can achieve this by introducing partner particles to the SM particles with couplings related as $\lambda_S = |\lambda_f|^2$ and different contributions to Higgs get cancelled. In more technical terms this procedure 'stabilizes' the Higgs mass and consequently provide an answer to the hierarchy problem.

3.2.2 Supersymmetric Field Theory

Supersymmetry is a transformation that turns a fermion to a boson and vice versa. In terms of quantum language we represent this as

$$Q|\text{Boson}\rangle = |\text{Fermion}\rangle, \qquad Q|\text{Fermion}\rangle = |\text{Boson}\rangle. \qquad (3.2.11)$$

According to the Coleman-Mandula theorem [34] the operator Q which can generate such transformations must be an anti-commuting spinor operator. Since spinors are complex, $Q^\dagger$ (the hermitian conjugate of Q) would also be a generator. We will discuss their properties in the following sections.

SUSY algebra

In field theory the word 'algebra' means the commutation (or anti-commutation) relations among the generators of the corresponding symmetry transformations. An example would be the anti-commutation relations of Pauli matrices which are the generators of

the $SU(2)$ group. Similarly there are Gell-Mann matrices for $SU(3)$ group and so on.

The symmetry operator Q's in eqn. 3.2.11 have two components and they transform as spin-1/2 objects. Therefore they must be described by a spin-1, 4-vector representation which is according to the Coleman-Mandula theorem, given by P_μ. This theorem also suggests that to avoid parity violating interactions due to the chiral fermions, these generators should satisfy these following commuting and anti-commuting relations. [33][1]

$$\{Q, Q^\dagger\} = P^\mu, \tag{3.2.12}$$

$$\{Q, Q\} = \{Q^\dagger, Q^\dagger\} = 0, \tag{3.2.13}$$

$$[P^\mu, Q] = [P^\mu, Q^\dagger] = 0, \tag{3.2.14}$$

Supermultiplets

The basic building block of supersymmetric algebra is the *supermultiplets* which are basically irreducible representation of single-particle states and contain both fermionic and bosonic components. These states are called *superpartners* of each other. There are two types of supermultiplets in renormalized field theory. A combination of Weyl fermion field and a complex scalar field is known as *chiral* or *matter* or *scalar* supermultiplet. Whereas a combination of spin-1/2 *gaugino* (fermionic superpartner of gauge bosons) and a spin-1 gauge bosons are known as *gauge* or *vector* supermultiplets. In forming these supermultiplets a very important criteria must be satisfied, the number of bosonic degrees of freedom (n_B) must be equal to the number of fermionic degrees of freedom (n_F), i.e. $n_B = n_F$. This is because, supersymmetry is a transformation between fermion and boson and naively each supermultiplet consists of a Weyl-fermion (with $n_F = 2$ for two helicity states) and a boson (real scalar with $n_B = 1$) which have different degrees of freedom, but a *symmetry* theory does not allow that to happen. For example, let's take

---

[1]Using the notation of ref. [33]

Names		spin 0	spin 1/2	$SU(3)_C,\ SU(2)_L,\ U(1)_Y$
squarks, quarks	Q	$(\widetilde{u}_L\ \ \widetilde{d}_L)$	$(u_L\ \ d_L)$	$(\mathbf{3},\ \mathbf{2}\ ,\ \frac{1}{6})$
($\times 3$ families)	$\overline{u}$	$\widetilde{u}_R^*$	$u_R^\dagger$	$(\overline{\mathbf{3}},\ \mathbf{1},\ -\frac{2}{3})$
	$\overline{d}$	$\widetilde{d}_R^*$	$d_R^\dagger$	$(\overline{\mathbf{3}},\ \mathbf{1},\ \frac{1}{3})$
sleptons, leptons	L	$(\widetilde{\nu}\ \ \widetilde{e}_L)$	$(\nu\ \ e_L)$	$(\mathbf{1},\ \mathbf{2}\ ,\ -\frac{1}{2})$
($\times 3$ families)	$\overline{e}$	$\widetilde{e}_R^*$	$e_R^\dagger$	$(\mathbf{1},\ \mathbf{1},\ 1)$
Higgs, higgsinos	H_u	$(H_u^+\ \ H_u^0)$	$(\widetilde{H}_u^+\ \ \widetilde{H}_u^0)$	$(\mathbf{1},\ \mathbf{2}\ ,\ +\frac{1}{2})$
	H_d	$(H_d^0\ \ H_d^-)$	$(\widetilde{H}_d^0\ \ \widetilde{H}_d^-)$	$(\mathbf{1},\ \mathbf{2}\ ,\ -\frac{1}{2})$

Table 3.2.1: Chiral supermultiplets in the Minimal Supersymmetric Standard Model. [33].

Names	spin 1/2	spin 1	$SU(3)_C,\ SU(2)_L,\ U(1)_Y$
gluino, gluon	$\widetilde{g}$	g	$(\mathbf{8},\ \mathbf{1}\ ,\ 0)$
winos, W bosons	$\widetilde{W}^\pm\ \ \widetilde{W}^0$	$W^\pm\ \ W^0$	$(\mathbf{1},\ \mathbf{3}\ ,\ 0)$
bino, B boson	$\widetilde{B}^0$	B^0	$(\mathbf{1},\ \mathbf{1}\ ,\ 0)$

Table 3.2.2: Gauge supermultiplets in the Minimal Supersymmetric Standard Model [33].

the chiral supermultiplet

$$\begin{pmatrix} \nu_{\mathrm{eL}} \\ e_{\mathrm{L}} \end{pmatrix} \text{ partnered by } \begin{pmatrix} \tilde{\nu}_{\mathrm{eL}} \\ \tilde{e}_{\mathrm{L}} \end{pmatrix}. \tag{3.2.15}$$

Here e_{L} and ν_{eL} are two Weyl-fermions, each with two degrees of freedom, so total degrees of freedom is four. Its superpartners are two complex scalars, $\tilde{\nu}_{\mathrm{eL}}$ and $\tilde{e}_{\mathrm{L}}$ each with two degrees of freedom. These supermultiplets are shown in Tables 3.2.1 and 3.2.2.

Since the supersymmetry is a symmetry between fermions and bosons, the particles within a supermultiplet must differ by their spin assignment as shown in Tables 3.2.1 and 3.2.2. The Standard Model fermions (quarks and leptons) are Weyl fermions with two helicity states ($n_F = 2$). Also they all are chiral in nature which means under the gauge group their left-handed part and right-handed part transform differently. This is the reason why they are placed in the Chiral supermultiplets. Clearly to maintain the

degrees of freedom their bosonic partners should have spin-0.

Nomenclature

It is a convention that the names of the superpartners of spin-0 particles of chiral supermultiplets start with a "s" in front, for scalars, and they are denoted by a tilde ($\tilde{\ }$) above their symbols. For example the superpartner of the SM left-handed quark (u_L) is a 'scalar quark' denoted by the symbol ($\tilde{u}_L$) and left-handed lepton (e_L) is a 'scalar lepton' denoted by the symbol ($\tilde{e}_L$). In general they are called *squarks* and *sleptons* or *sfermions* all together.

The similar nomenclature for a spin-1/2 superpartner is to add "ino" in the end of the known SM particles. For example the spin-1/2 superpartner of the Higgs particle in the chiral supermultiplet is called *higgsino*, the superpartner of gluon in the gauge supermultiplet is *gluino* etc.

SUSY Lagrangian

After establishing the particle content of the theory and the supermultiplets, in this section we will briefly discuss how to build a supersymmetric Lagrangian.

Chiral Lagrangian for free fields

Let's first concentrate on the Lagrangian of a chiral supermultiplets. In writing a Lagrangian we must remember a basic thing that the number of fields/degrees of freedom, between the bosonic ϕ fields and the fermionic ψ fields, should be the same in a transformation equation (between fermion and boson).

Chiral supermultiplets usually consist of a single left-handed two-component Weyl fermion ψ and a two-degree-of-freedom bosonic field which is given by a complex (charged) scalar field ϕ to maintain the same degrees of freedom. Therefore the simplest action must

consists of kinetic energy terms for each of them as [33]

$$S = \int d^4x (\mathcal{L}_{scalar} + \mathcal{L}_{fermion}), \tag{3.2.16}$$

$$\mathcal{L}_{scalar} = -\partial^\mu \phi^* \partial_\mu \phi, \quad \mathcal{L}_{fermion} = i\psi^\dagger \bar{\sigma}^\mu \partial_\mu \psi. \tag{3.2.17}$$

This is known as the massless, non-interacting *Wess-Zumino model.*

Also according to 3.2.11 a scalar boson field ϕ turn into a fermion field ψ_α under SUSY transformation. Therefore we can start by guessing what might be that transformation. We can assume that the change in ϕ is related to the change of ψ as [35]

$$\text{'change in } \phi = \text{parameter } \epsilon \times \text{other field } \psi'. \tag{3.2.18}$$

On the LHS of eqn. 3.2.18, we have a Lorentz invariant spin-0 field. Therefore for the RHS to be comparable with the LHS we must form a Lorentz invariant combination of ψ and the parameter ϵ. The simplest way to do this is to declare the ϵ as a ψ- (or L-) type spinor and use the invariant product that gives [35]

$$\delta\phi = \epsilon^T(-i\sigma_2)\psi = \epsilon\psi. \tag{3.2.19}$$

Therefore we can write the required transformations as

$$\delta\phi = \epsilon\psi, \quad \delta\phi^* = \epsilon^\dagger \psi^\dagger. \tag{3.2.20}$$

Using 3.2.20 we can write the scalar part of the Lagrangian

$$\delta\mathcal{L}_{scalar} = -\epsilon\partial^\mu\psi\partial_\mu\phi^* - \epsilon^\dagger\partial^\mu\psi^\dagger\partial_\mu\phi \tag{3.2.21}$$

Now we need to know what the corresponding $\delta\psi$ might be. By similar analogy as

for the $\delta\phi$ case, we can say that this has to be something like

$$\delta\psi \sim \text{product of } \epsilon \text{ and } \phi \tag{3.2.22}$$

Looking at 3.2.22 carefully we find that the LHS has mass dimension $\mathrm{M}^{3/2}$, whereas the RHS has dimensions $\mathrm{M}^{-1/2+1} = \mathrm{M}^{1/2}$. Thus the RHS needs an introduction of something with dimensions M^1. Since we are considering a massless non-interacting model the only possibility is the gradient operator ∂_μ or more conveniently the momentum operator $i\partial_\mu$. But to maintain the space-time index we need to contract the RHS. Therefore we can write

$$\delta\psi = (i\sigma^\mu\partial_\mu\phi)\,\epsilon \tag{3.2.23}$$

where σ^μ is given by

$$\sigma^\mu \equiv (1, \boldsymbol{\sigma}), \quad \bar{\sigma}^\mu = (1, -\boldsymbol{\sigma}). \tag{3.2.24}$$

and $\boldsymbol{\sigma} \equiv (\sigma_x, \sigma_y, \sigma_z)$ are the 2×2 Pauli Matrices. The σ^μ act on the 2-component column ϵ to give a 2-component column, but the RHS does not transform as a ψ-type spinor. In order to transform both sides of 3.2.23 similar way the transformations need to be of the form

$$\delta\psi_\alpha = -iA(\sigma^\mu\epsilon^\dagger)_\alpha\,\partial_\mu\phi, \qquad \delta\psi^\dagger_{\dot\alpha} = iA(\epsilon\sigma^\mu)_{\dot\alpha}\,\partial_\mu\phi^*. \tag{3.2.25}$$

where A is a constant and usually to be determined from the condition that $\mathcal{L}$ is invariant under both 3.2.20 and 3.2.25. With these transformations we are able to write the fermionic part of the Lagrangian as

$$\begin{aligned}
\delta\mathcal{L}_{\text{fermion}} &= -\epsilon\partial^\mu\psi\,\partial_\mu\phi^* - \epsilon^\dagger\partial^\mu\psi^\dagger\,\partial_\mu\phi \\
&\quad -\partial_\mu\left(\epsilon\sigma^\nu\bar{\sigma}^\mu\psi\,\partial_\nu\phi^* - \epsilon\psi\,\partial^\mu\phi^* - \epsilon^\dagger\psi^\dagger\,\partial^\mu\phi\right).
\end{aligned} \tag{3.2.26}$$

Comparing with 3.2.21 we find that first two terms of 3.2.26 gets canceled and the rest terms are a total derivative which contribute nothing. This leaves the action invariant.

Now, ϕ being single complex field with two degrees of freedom don't match up with ψ which is a two-component complex field with four degrees of freedom. Therefore to make sure that the number of fermionic and bosinic degrees of freedom are same and SUSY algebra is satisfied both classically (on-shell) and quantum mechanically (off-shell) we need to introduce two more real scalar degrees of freedom. This purpose is solved by introducing an extra book-keeping term known as the "F-terms". They are complex scalar fields, denoted by F and don't have any kinetic terms. They are known as 'auxiliary' field with the dimension $[\text{mass}]^2$ and the Lagrangian density given by

$$\mathcal{L}_{\text{auxiliary}} = F^*F. \tag{3.2.27}$$

Therefore the free part of the chiral supermultiplet Lagrangian consist of a complex scalar field ϕ, a Weyl Fermion ψ and an auxiliary complex scalar F is given by

$$\mathcal{L}_{\text{free}} = -\partial^\mu \phi^{*i}\partial_\mu \phi_i + i\psi^{\dagger i}\bar{\sigma}^\mu \partial_\mu \psi_i + F^{*i}F_i, \tag{3.2.28}$$

where superscript i runs over all gauge and flavor degrees of freedom.

Chiral Lagrangian for interacting fields

In this section we try to find out the most general interactions of particles that are placed under the chiral supermultiplet. Since 3.2.28 is invariant under the supersummetry transformations

$$\delta\phi_i = \epsilon\psi_i, \qquad \delta\phi^{*i} = \epsilon^\dagger \psi^{\dagger i} \tag{3.2.29}$$

$$\delta(\psi_i)_\alpha = -i(\sigma^\mu \epsilon^\dagger)_\alpha \partial_\mu \phi_i + \epsilon_\alpha F_i, \quad \delta(\psi^{\dagger i})_{\dot\alpha} = i(\sigma^\mu \epsilon)_{\dot\alpha}\partial_\mu \phi^{*i} + \epsilon^\dagger_{\dot\alpha} F^{*i} \tag{3.2.30}$$

$$\delta F_i = -i\epsilon^\dagger \bar{\sigma}^\mu \partial_\mu \psi_i, \quad \delta F^{*i} = i\epsilon\partial_\mu \psi^{\dagger i}\bar{\sigma}^\mu \tag{3.2.31}$$

we need to find out most general renormalizable interactions that are consistent with these transformations. The only possible renormalizable (mass dimension $\lesssim 4$) terms that can be included within the interaction Lagrangian are

$$\mathcal{L}_{\text{int}} = \left(-\frac{1}{2}W^{ij}\psi_i\psi_j + W^i F_i + x^{ij}F_iF_j\right) + \text{c.c.} - U(\phi, \phi^*), \tag{3.2.32}$$

where x^{ij}, W^{ij}, W^i and U are polynomials in the scalar fields ϕ_i, ϕ^{*i} and has mass dimensions 0, 1, 2 and 4 respectively. The terms those are generated due to the action of supersymmetric transformation equations 3.2.29-3.2.31 on $x^{ij}F_iF_j$ and $U(\phi, \phi^*)$, can't be canceled by the supersymmetry transformation of any other term in the Lagrangian and therefore those terms can be dropped. therefore the final expression for the interacting Lagrangian becomes

$$\mathcal{L}_{\text{int}} = \left(-\frac{1}{2}W^{ij}\psi_i\psi_j + W^i F_i +\right) + \text{c.c.} \tag{3.2.33}$$

W^{ij} is a holomorphic function of chiral supermultiplets ϕ_k and can be expressed as

$$W^{ij} = M^{ij} + y^{ijk}\phi_k \tag{3.2.34}$$

where M^{ij} is a symmetric mass matrix of fermion fields and y^{ijk} is a symmetric (under interchange of i, j, k) Yukawa coupling between a scalar ϕ_k and two fermions $\psi_i\psi_j$. It is also convenient to write

$$W^{ij} = \frac{\delta^2}{\delta\phi_i\delta\phi_j}W \tag{3.2.35}$$

where

$$W = \frac{1}{2}M^{ij}\phi_i\phi_j + \frac{1}{6}y^{ijk}\phi_i\phi_j\phi_k, \tag{3.2.36}$$

is called the *superpotential* and is an important object of SUSY field theory in a sense that most matter interactions of chiral supermultiplets can be expressed in terms of this single function W. Even the auxiliary fields can also be expressed in terms of W as

follows:

$$F_i = -W_i^*, \qquad\qquad F^{*i} = -W^i \qquad\qquad (3.2.37)$$

where

$$W^i = \frac{\delta W}{\delta \phi_i} = M^{ij}\phi_j + \frac{1}{2}y^{ijk}\phi_j\phi_k. \qquad\qquad (3.2.38)$$

Finally we can write the chiral supermultiplets Lagrangian density as

$$
\begin{aligned}
\mathcal{L}_{\text{chiral}} \;=\; & \partial^\mu\phi^{*i}\partial_\mu\phi_i - V(\phi,\phi^*) + i\psi^{\dagger i}\overline{\sigma}^\mu\partial_\mu\psi_i - \frac{1}{2}M^{ij}\psi_i\psi_j - \frac{1}{2}M_{ij}^*\psi^{\dagger i}\psi^{\dagger j} \\
& -\frac{1}{2}y^{ijk}\phi_i\psi_j\psi_k - \frac{1}{2}y_{ijk}^*\phi^{*i}\psi^{\dagger j}\psi^{\dagger k}.
\end{aligned}
\qquad (3.2.39)
$$

where the scalar potential in terms of the superpotential is given by

$$
\begin{aligned}
& V(\phi,\phi^*) = W^k W_k^* = F^{*k}F_k = \\
& M_{ik}^* M^{kj}\phi^{*i}\phi_j + \frac{1}{2}M^{in}y_{jkn}^*\phi_i\phi^{*j}\phi^{*k} + \frac{1}{2}M_{in}^*y^{jkn}\phi^{*i}\phi_j\phi_k + \frac{1}{4}y^{ijn}y_{kln}^*\phi_i\phi_j\phi^{*k}\phi^{*l} \;\; (3.2.40)
\end{aligned}
$$

Gauge supermultiplet Lagrangian

Similar as the chiral supermultiplets, gauge supermultiplets consist of a Weyl fermion gaugino λ^a and a vector gauge boson field A_μ^a with a representing the adjoint representation of gauge groups. Clearly, for off-shell situation the fermion has four real degrees of freedom due to its two complex components, but the massless boson has two. To compensate that, similar to the chiral case an auxiliary field is introduced. This is called the "D-term". Like the "F-term" it also has mass dimension 2 and without any kinetic term, but it is real in this case. Therefore the Lagrangian density for a gauge supermultiplet is given by

$$\mathcal{L}_{\text{gauge}} = -\frac{1}{4}F_{\mu\nu}^a F^{\mu\nu a} + i\lambda^{\dagger a}\overline{\sigma}^\mu\nabla_\mu\lambda^a + \frac{1}{2}D^a D^a, \qquad\qquad (3.2.41)$$

where

$$F_{\mu\nu}^a = \partial_\mu A_\nu^a - \partial_\nu A_\mu^a - g f^{abc} A_\mu^b A_\nu^c \tag{3.2.42}$$

is the Yang-Mills field strength, and

$$\nabla_\mu \lambda^a = \partial_\mu \lambda^a - g f^{abc} A_\mu^b \lambda^c \tag{3.2.43}$$

represents the covariant derivative of the propagating gaugino field in the adjoint representation.

3.2.3   The Minimal Supersymmetric Standard Model(MSSM)

In a renormalizable supersymmetric field theory, the interactions and masses of all particles are determined by their gauge transformation properties and by the superpotential term W. By construction, W has to be a holomorphic function of the complex scalar fields ϕ_i, which transform into left-handed Weyl fermions under supersymmetry. Equivalently, W is said to be a function of chiral superfields containing the bosonic, fermionic, and auxiliary fields within the corresponding supermultiplet, for example $\Phi_i \supset (\phi_i, \psi_i, F_i)$.

The superpotential term in the MSSM is given by [33]

$$\begin{aligned}
W_{MSSM} &= \bar{u} y_u Q H_u - \bar{d} y_d Q H_d - \bar{e} y_e L H_d + \mu H_u H_d \\
&= y_u^{ij} \bar{u}_i Q_j \cdot H_u - y_d^{ij} \bar{d}_i Q_j \cdot H_d - y_e^{ij} \bar{e}_i L_j \cdot H_d + \mu H_u \cdot H_d.
\end{aligned} \tag{3.2.44}$$

where H_u, H_d, Q, L, $\bar{u}$, $\bar{d}$, $\bar{e}$ are chiral superfields of chiral supermultiplets in Table 3.2.1. y_u, y_d, y_e are 3×3 Yukawa coupling matrices in family space. For convenience we have suppressed all gauge [$SU(3)_C$ color and $SU(2)_L$ weak isospin] and family indices in eqn. (3.2.44).

An interesting fact to notice here is the presence of two Higgs doublet instead of one that is present in the SM. The reason is the following. In SUSY to give mass to the up-type quarks we need the term $\bar{u}QH_u$, similar to the SM, but to give mass to the down-type quarks we can not use SM like term $\bar{u}QH_d^*$. Since the superpotential must be a holomorphic function of the chiral supermultiplets, this sort of complex conjugation is not allowed. Therefore, we need to introduce another chiral supermultiplet H_d with similar quantum numbers as $\bar{u}QH_d^*$.

Knowing the superpotential we can calculate the scalar potential similar to eqn. 3.2.40 and proceed with all our further analysis.

3.3   Supersymmetry Breaking

The supersymmetry is a broken symmetry for several reasons. The most convincing reason is the non-existence of several supersymmetric particles which should have been easily found by now if SUSY were a perfect symmetry. For example, if supersymmetry were not broken, then there would have been selectrons $\tilde{e}_L$ and $\tilde{e}_R$ with masses equal to the electron $m_e \sim 0.511$ MeV. Similarly there should have been massless gluino and photino analogous to the SM gluon and photon. There absence is an experimental indication of broken SUSY. Another indication of SUSY breaking comes from a theoretical point of view, the motivation of the hierarchy problem: supersymmetric field theory needs two complex scalar fields for each Standard Model Dirac fermion to cancel the quadratically divergent contribution due to a very high cut-off scale, Λ_{UV}^2. This sort of cancellation also demands that the corresponding dimensionless couplings of scalar and fermion should be related (for example $\lambda_S \sim |\lambda_f|^2$). In unbroken supersymmetry limit there are no radiative corrections to any mass parameter and thus the Higgs mass and consequently the SM is stable. Therefore if we still want the broken supersymmetry to provide a solution to the hierarchy problem we should not disturb the relationships between dimensionless

couplings that hold in an unbroken supersymmetric theory. That's why we need to break supersymmetry explicitly, means to add some terms by hand without disturbing the basic idea of unbroken supersymmetry. This is known as "soft" SUSY breaking. We shall discuss these concepts in the following subsections.

3.3.1 Spontaneous SUSY Breaking

In quantum field theory a symmetry is spontaneously broken if a field which is not invariant under this symmetry gets a non-vanishing vacuum expectation value (vev). Symbolically, if we denote such a field by ϕ', the above requirement means $\langle 0|\phi'(x)|0\rangle \neq 0$. The fact that the field ϕ' is not invariant, implies that it must belong to a symmetry multiplet which also include other fields and also it can be expressed as

$$\phi'(x) = i[Q, \phi(x)] \tag{3.3.1}$$

where Q is a generator of the symmetry group, and ϕ is a field belongs to the symmetry multiplet. Therefore we have

$$\langle 0|\phi'|0\rangle = \langle 0|i[Q, \phi]|0\rangle = i[\langle 0|Q\phi - \phi Q|0\rangle] \neq 0. \tag{3.3.2}$$

as the condition for a field to have non-zero vev and thus a spontaneously broken symmetry.

Usually a vacuum state $|0\rangle$ is defined as a state on which the symmetry generator acts to give 0, i.e $Q|0\rangle = 0$. Looking at 3.3.2 we find that if we take $Q|0\rangle = 0$ we violate 3.3.2, the fundamental requirement of spontaneously broken symmetry. Therefore we need to assume that the vacuum is not invariant under the symmetry if that symmetry to be broken spontaneously. In the case of SUSY, this requirement means that we need these

relations [35]

$$Q_\alpha |0\rangle \neq 0, \quad Q_{\dot{\alpha}}^\dagger |0\rangle \neq 0, \tag{3.3.3}$$

to be satisfied for the SUSY generators $Q_\alpha, Q_{\dot{\alpha}}$.

Let us now discuss the significance of 3.3.3 for the case of spontaneous symmetry breaking in SUSY. Equation 3.2.12 can be written more explicitly as [35]

$$\{Q_\alpha, Q_{\dot{\alpha}}^\dagger\} = -2(\sigma^\mu)_{ab} P_\mu. \tag{3.3.4}$$

where

$$\sigma^0 = \overline{\sigma}^0 = \begin{pmatrix} 1 & 0 \\ 0 & 1 \end{pmatrix}, \qquad \sigma^1 = -\overline{\sigma}^1 = \begin{pmatrix} 0 & 1 \\ 1 & 0 \end{pmatrix},$$

$$\sigma^2 = -\overline{\sigma}^2 = \begin{pmatrix} 0 & -i \\ i & 0 \end{pmatrix}, \qquad \sigma^3 = -\overline{\sigma}^3 = \begin{pmatrix} 1 & 0 \\ 0 & -1 \end{pmatrix}. \tag{3.3.5}$$

Therefore we have

$$Q_1 Q_1^\dagger + Q_1^\dagger Q_1 = -2(\sigma^\mu)_{11} P_\mu = 2(P_0 + P_3)$$

$$Q_2 Q_2^\dagger + Q_2^\dagger Q_2 = -2(\sigma^\mu)_{22} P_\mu = 2(P_0 - P_3).$$

It follows that

$$P_0 = \frac{1}{4}(Q_1 Q_1^\dagger + Q_1^\dagger Q_1 + Q_2 Q_2^\dagger + Q_2^\dagger Q_2) = H, \tag{3.3.6}$$

where H is the Hamiltonian of the theory considered. Finally we get

$$
\begin{aligned}
\langle 0|H|0\rangle &= \frac{1}{4}(\langle 0|Q_1 Q_1^\dagger|0\rangle + \langle 0|Q_1^\dagger Q_1|0\rangle + \ldots) \\
&= \frac{1}{4}(\ |(Q_1^\dagger|0\rangle)|^2 + |(Q_1|0\rangle)|^2 + |(Q_2^\dagger|0\rangle)|^2 + |(Q_2|0\rangle)|^2) \\
&> 0,
\end{aligned}
\qquad (3.3.7)
$$

where this inequality is a direct consequence of 3.3.3. A very important conclusion can be drawn from 3.3.7: *For SUSY to be broken spontaneously, the vacuum energy must be positive.* Which also implies that, when SUSY is exact, means $Q_\alpha|0\rangle = Q_{\dot{\alpha}}^\dagger|0\rangle = 0$, we have $\langle 0|H|0\rangle = 0$ - the vacuum energy of a (globally) SUSY-invariant theory is zero.

After deriving the conditions for spontaneously breaking of SUSY we can look for the fields ϕ' which satisfies 3.3.2. Let's start with chiral supermultiplets which contain a scalar, a Weyl fermion and an auxiliary field F-term. The corresponding SUSY transformations are given by 3.2.29, 3.2.30 and 3.2.31 respectively. Looking at the RHS of these three equations we find $\langle 0|\psi|0\rangle \neq 0$ is not possible because ψ is a spinor and such a vev is not Lorentz invariant. $\langle 0|\partial_\mu \phi|0\rangle \neq 0$ is also not possible because the scalar ϕ is assumed to be constant in the vacuum. Therefore the only option we have is to consider

$$
\langle 0|F_i|0\rangle \neq 0 \qquad (3.3.8)
$$

which is known as 'F-term SUSY breaking'. Similarly for the gauge supermultiplets we can only have a non-zero vev via

$$
\langle 0|D_\alpha|0\rangle \neq 0 \qquad (3.3.9)
$$

which is known as 'D-term SUSY breaking'.

Equations 3.3.8 and 3.3.9 tell us that if there exist any state in which all F_i and D_a vanish then it will imply that SUSY is not spontaneously broken in the true ground state. In other words, for guaranteed supersymmetry breaking we need to look for scenarios

where $F_i = 0$ and $D_a = 0$ cannot both be simultaneously satisfied for any values of the fields.

3.3.2 'Soft' SUSY breaking

For low-energy effective theories, usually we just add terms to supersymmetric Lagrangians which break supersymmetry explicitly. These explicit SUSY breaking terms of supersymmetry are called "soft" breakings because they have positive mass dimension, for example '$M^2\phi^2$', '$M\phi^3$', etc. On the other hand '$\frac{\phi^5}{M}$' is not a "soft" term. Another reason why they are called 'soft' is that they don't introduce new quadratic divergences into the relations between the dimensionless coupling constants of scalars and fermions and help stabilizing the mass hierarchy issue of SUSY.

When we think about the terms which can be considered as 'soft' SUSY breaking terms, there are actually very limited options. These following terms can be considered:

(a) Gaugino masses for each gauge group:

$$-\frac{1}{2}(M_3\tilde{g}^\alpha \cdot \tilde{g}^\alpha + M_2\tilde{W}^\alpha \cdot \tilde{W}^\alpha + M_1\tilde{B} \cdot \tilde{B} + \text{h.c.}) \tag{3.3.10}$$

where for the gluino (g) term α runs from 1 to 8 and for wino (W) term it runs from 1 to 3. The dot here signifies the Lorentz invariant spinor product and (B) stands for bino). These quantities are allowed because '$\widetilde{W} \cdot \widetilde{W}$' don't include any derivatives and are invariant under SU(2) transformations; similarly for the gluinos and the bino.

(b) Squark (mass)^2 terms:

$$-m^2_{\tilde{Q}ij}\tilde{Q}^\dagger_i \cdot \tilde{Q}_j - m^2_{\tilde{u}ij}\tilde{u}^\dagger_i\tilde{u}_j - m^2_{\tilde{d}ij}\tilde{\bar{d}}^\dagger_i\tilde{\bar{d}}_j, \tag{3.3.11}$$

where i and j represent the generations.

(c) Slepton (mass)^2 terms:

$$- m^2_{\tilde{L}ij} \tilde{L}^\dagger_i \cdot \tilde{L}_j - m^2_{\tilde{e}ij} \tilde{e}^\dagger_i \tilde{e}_j, \tag{3.3.12}$$

are allowed if i, j are family indices and m^2_{ij}'s are Hermitian mass matrices in family space.

(d) Higgs (mass)^2 terms:

$$- m^2_{H_u} H^\dagger_u \cdot H_u - m^2_{H_d} H^\dagger_d \cdot H_d - (b H_u \cdot H_d + \text{h.c.}) \tag{3.3.13}$$

where

$$H^\dagger_u \cdot H_u = |H^+_u|^2 + |H^0_u|^2 \tag{3.3.14}$$

and similarly for $H^\dagger_d \cdot H_d$, while

$$H_u \cdot H_d = H^+_u H^-_d - H^0_u H^0_d. \tag{3.3.15}$$

The b term in (3.3.13) is similar to the SUSY-invariant μ term, but it involves only Higgs, not the Higgsinos and hence can be considered as a SUSY-breaking term.

(e) Triple scalar couplings

$$- a^{ij}_u \tilde{\bar{u}}_i \tilde{Q}_j \cdot H_u + a^{ij}_d \tilde{\bar{d}}_i \tilde{Q}_j \cdot H_d + a^{ij}_e \tilde{\bar{e}}_i \tilde{L}_j \cdot H_d + \text{h.c.} \tag{3.3.16}$$

$a_{u,d,e}$ is a complex 3×3 matrix in family space, with dimensions of [mass].

Combining 3.3.10-3.3.16 we get the most general soft supersymmetry-breaking Lagrangian consistent with gauge symmetry.

The interesting fact about these soft terms are that they introduce many new parameters apart from the SM parameters. These terms also break SUSY explicitly, but preserve the electroweak (EW) symmetry which is a problem because to generate the

SM particles EW symmetry needs to be broken. Therefore it is expected that to avoid fine-tuning at least some of these SUSY-breaking parameters must have values not too far from the EW symmetry breaking scale.

3.4 Different SUSY breaking mediation mechanisms

It is argued that supersymmetry is a broken symmetry, but how this breaking happen is not known to us. It is a popular idea to think that the breaking of symmetry is happening at presumably some very high energy scale ($\sim M_{\text{Planck}}$), ('hidden sector') and the effect is being 'communicated' to the low-energy level ('visible sector') accessible to modern day collider experiments. To communicate between these two sectors we need some 'mediators'. Some details of those mediators, their mediation mechanism and how they give rise to the soft SUSY breaking terms will be discussed in this section.

3.4.1 The need for a separate supersymmetry-breaking sector

A careful study of F-term and D-term SUSY breaking revels that a supersymmetry-breaking order parameter doesn't belong to any of the MSSM supermultiplets because of two reasons. First, a D-term vev for $U(1)_Y$ leads to an unacceptable spectrum. Second, there is no gauge singlet whose F -term could develop a vev. Therefore to break the supersymmetry spontaneously the MSSM needs to be extended to accommodate the effects that are responsible for SUSY breaking and how these effects are communicating to the MSSM particles.

It is assumed that supersymmetry breaking happens in a 'hidden sector (high-energy level) rather than in a 'visible sector (low-energy level) where MSSM particles exist. A 'hidden sector' usually consists of singlets under the SM gauge group and don't feel either strong or electro-weak force. Consequently their interactions can't be experienced via the interactions mediated by the usual SM gauge bosons. That is why they are called 'hidden

sector'.

3.4.2 Some general facts about hidden sector SUSY breaking

The visible sector and the hidden sector share 'some interactions' though those are suppressed by powers more than Planck scale. Since Supergravity (SUGRA) couples to all fields, we can safely assume that two sectors are connected by it. This was the motivation of "*gravity-mediated*" or "*Planck-scale-mediated supersymmetry breaking*" (PMSB) supersymmetry breaking. In this scenario, if supersymmetry is broken in the hidden sector by a F-term VEV $\langle F \rangle$, by dimensional analysis the soft terms in the visible sectors are roughly given by

$$m_{\text{soft}} \sim \frac{\langle F \rangle}{M_P}, \tag{3.4.1}$$

where M_P is the Planck mass. The reason we have such form of *soft* masses like eqn. 3.4.1 is, we know that m_{soft} must vanish in the limit $\langle F \rangle \to 0$ where supersymmetry is unbroken. This is also true in the limit $M_P \to \infty$ (equivalent to $G_{Newton} \to 0$) where gravity becomes irrelevant. Clearly from eqn. 3.4.1 we find that the scale associated with the origin of supersymmetry breaking in the hidden sector should be roughly $\sqrt{\langle F \rangle} \sim 10^{10}$ or 10^{11} GeV.

Another possibility of hidden sector SUSY breaking is the flavor-blind mediating interactions like electroweak and QCD gauge interactions where the mediators are gauge bosons like Z or W. This is known as "*gauge-mediated supersymmetry breaking*" or GMSB. In this scenario the mediator particles are some new chiral supermultiplets that couple the visible and hidden sector field generating SUSY-breaking VEV. They create some loop-diagrams which generate the MSSM soft-terms. Then again from dimensional analysis, the MSSM soft terms can have the form

$$m_{\text{soft}} \sim \frac{\alpha}{4\pi} \frac{\langle F \rangle}{M_{\text{mess}}} \tag{3.4.2}$$

where the $\alpha/4\pi$ is the loop factor coming from the Feynman diagrams involving gauge interactions and M_{mess} is the messenger fields mass scale. Similar analysis as PMSB shows that to generate the correct m_{soft} masses, the SUSY breaking scale would be $\sqrt{\langle F \rangle} \sim 10^4$ GeV.

3.4.3 Anomaly mediation of SUSY breaking

Now from a low-energy point of view, it is a common practice to parameterize the most general effects of the unknown physics of the high scale by higher dimensional operators suppressed by relevant powers of the Planck scale M_P. When we write down the most general interactions between a singlet field in the hidden sector there exist some terms that are allowed by all symmetries and can produce unacceptable flavor-changing neutral currents (FCNCs'). This is known as the 'SUSY flavor problem'.

A solution to this problem was proposed by Randall and Sundrum [37]. There are several assumptions made for this hidden sector mediation mechanism to work such as:

- There are n ($\gtrsim 1$) extra dimensions compactified with a radius R $>> 1/M_*$, where M_* is the (4 +n)-dimensional Planck scale.

- The SUSY breaking hidden sector and the observable sector with all SM particles are localized on a $(3 + 1)$-dimensional subspace in extra dimensions or 3-brane in higher dimensions.

- For simplicity the compactified space can be taken as a symmetric torus with radius R so that the distance between the two sectors can be $\sim \pi R$. This is the most natural choice for the separation of the 3-branes.

- The only light (below M_*) fields that communicate the supersymmetry breaking effects between the branes (or equivalently in the bulk) are SUperGravity (SUGRA) fields.

Assuming only renormalizable couplings in the observable sector do not give rise to soft SUSY breaking terms, but they are generated at the loop level from conformal anomaly. That is why this mechanism is known as anomaly mediated supersymmetry breaking (AMSB). In anomaly mediation therefore the soft SUSY breaking parameters are determined by $m_{3/2}$ and anomalous dimensions at the electroweak scale. Specifically the contribution to the gaugino and squark masses are given by

$$m_\lambda = \frac{\beta(g^2)}{2g^2}m_{3/2}, \quad m_{\tilde{Q}}^2 = -\frac{1}{4}\frac{d\gamma_Q}{d\ln\mu}m_{3/2}^2 \qquad (3.4.3)$$

respectively, where

$$\beta(g^2) = \frac{dg^2}{d\ln\mu}, \quad \gamma_Q = \frac{d\ln Z_Q}{d\ln\mu} \qquad (3.4.4)$$

are the gauge beta function and matter field anomalous dimensions [38] respectively. g denotes the Yukawa couplings. Eqn. 3.4.3 reveals that scalar and gaugino masses are of the same order

$$m_\lambda \sim m_{\tilde{Q}} \sim M_{\text{SUSY}} = \frac{m_{3/2}}{16\pi^2} \qquad (3.4.5)$$

which hold for any scenario with additional suppressions between the hidden and observable sectors.

Problem of anomaly mediation

The serious problem of the anomaly mediation is the negative slepton masses. The signs of the soft mass terms are determined by the anomalous dimensions which for a chiral field with 1-loop contributions is given by

$$\gamma \sim \frac{1}{16\pi^2}\big(-\lambda^2 + g^2\big). \qquad (3.4.6)$$

Therefore the scalar masses are given by

$$
\begin{aligned}
m^2 \quad &\sim \quad -m_{3/2}^2 \left(\frac{\partial \gamma}{\partial \lambda} \beta_\lambda + \frac{\partial \gamma}{\partial g} \beta_g \right) \\
&\sim \quad + \left(\frac{m_{3/2}}{16\pi^2} \right)^2 [+\lambda(\lambda^3 - \lambda g^2) - g(\pm g^3)]. \quad (3.4.7)
\end{aligned}
$$

for $\beta_g \sim \pm g^3/16\pi^2$ and $\beta_\lambda \sim (\lambda^3 - \lambda g^2)/16\pi^2$. Clearly when the Yukawa couplings are negligible ($g \to 0$), the asymptotically free gauge group ($\lambda = +$) gives positive sign for scalar mass-squared, but non asymptotically free gauge group ($\lambda = -$) gives negative sign for scalar mass-squared. For the case of leptons, they are charged under the non asymptotically free gauge group $SU(2)_W \times U(1)_Y$ and also their Yukawa couplings are small in the MSSM. Therefore the sleptons get negative masses.

3.4.4 Z' mediation of SUSY breaking

Z' mediation of supersymmetry (SUSY) breaking is a mediation mechanism in which both the hidden and the visible sectors are charged under a new $U(1)'$ gauge interaction. These two sectors don't possess any renormalized coupling between them. A supersymmetry breaking Z'-ino mass term, $M_{\tilde{Z}'}$, is generated due to the $U(1)'$ coupling to the hidden sector. The observable sector fields realize the SUSY breaking effects through their couplings to $U(1)'$ [39]. The scenario has been illustrated by Fig 3.4.1.
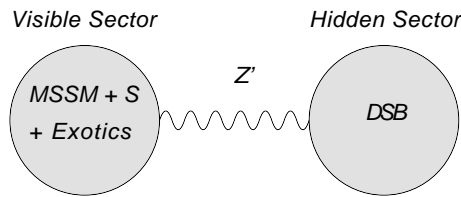

Figure 3.4.1: Schematic diagram of Z'-mediated supersymmetry breaking [39].

In this set up, the general assumptions are the following [39]:

- The gauge interaction is unbroken in the hidden sector

- Only visible sector fields, which do not participate in supersymmetry breaking, are charged under both group hypercharge $U(1)_Y$ and the new $U(1)'$.

- At a scale Λ_S, SUSY is broken and a Z' gaugino mass, $M_{\tilde{Z}'}$, is generated.

- The μ parameter is replaced by an effective term λS where S is a SM singlet charged under the $U(1)'$.

- To make the model anomaly free 'exotics' are included. These type of particles are usual in string theory constructions.

With this set up the superpotential becomes [39, 40]

$$
\begin{aligned}
W &= y_u H_u Q u^c + y_d H_d Q d^c + y_e H_d L e^c \\
&+ y_\nu H_u L \nu^c + \lambda S H_u H_d \\
&+ S \left(\sum_{i=1}^{n_D} y_{D_i} D_i D_i^c + \sum_{j=1}^{n_E} y_{E_j} E_j E_j^c \right),
\end{aligned}
\tag{3.4.8}
$$
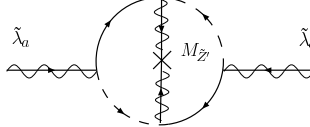
where n_D and n_E are the pairs of triplet and singlet pairs of exotics.

At the hidden sector, at SUSY breaking scale Λ_S the Z'-gaugino mass is generated. Other particles get masses in different ways under the Z' mediation mechanism. The scalar soft masses get mass at one-loop order and are proportional to the Z' coupling and $U(1)'$ charges of f_i charges and thus can be expressed as [40],

$$
m_{\tilde{f}_i}^2 \sim \frac{g_{Z'}^2 Q_{f_i}^2}{16\pi^2} M_{\tilde{Z}'}^2 \log\left(\frac{\Lambda_S}{M_{\tilde{Z}'}} \right).
\tag{3.4.9}
$$

There are two kinds of gaugino masses when we consider this particular $U(1)'$ extension of Minimal Supersymmetric Standard Model (MSSM). (i) MSSM gaugino and (ii) $U(1)'$ gauginos or Z'-ino. The $SU(3)_C \times SU(2)_L \times U(1)_Y$ gaugino masses can only be generated

at 2-loop level because they do not directly couple to the $U(1)'$,

$$M_a \quad \sim \quad \frac{g_{Z'}^2 g_a^2}{(16\pi^2)^2} M_{\tilde{Z}'} \log\left(\frac{\Lambda_S}{M_{\tilde{Z}'}}\right), \tag{3.4.10}$$

where g_a is the gauge coupling for the gaugino $\tilde{\lambda}_a$, and the internal line is the sum over the chiral supermultiplets charged under the ath gauge group [40].

Problem of Z' mediation

From eqns.3.4.9 and 3.4.10 we find the ratio of scalar and gaugino masses in the Z' mediation mechanism to be

$$\frac{m_{\tilde{f}_i}}{M_a} \sim \frac{M_{\tilde{Z}'}}{4\pi} / \frac{M_{\tilde{Z}'}}{(4\pi)^4} = (4\pi)^3 \sim 1000. \tag{3.4.11}$$

From the direct searches at the Large Electron Positron (LEP) collider we know the electroweak-ino or M_a should have mass greater than 100 GeV. Therefore we have two options. First is applying this lower bound of gaugino, from eqn. 3.4.10 we get

$$M_{\tilde{Z}'} \log\left(\frac{\Lambda_S}{M_{\tilde{Z}'}}\right) \sim 10^4 \text{ TeV} \tag{3.4.12}$$

and

$$m_{\tilde{f}_i} \sim \frac{(4\pi)^3}{g_{z'} g_a^2} M_a \sim 100 \text{ TeV}, \tag{3.4.13}$$

which means scalars are extremely heavy and a significant amount of fine-tuning is needed to produce them at the electroweak scale.

The other option is considering scalars at the EW scale ($\sim 100 - 1000$ GeV). Then

the gauginos become too light and they must acquire mass from other mechanism such as anomaly mediation mechanism.

3.4.5 SUSY breaking combining anomaly and Z' mediation

Z' gaugino and anomaly mediation are similar in the sense that both are flavor diagonal. Also, comparing the soft mass spectrum of both, it is clear that the scale of the soft parameters is set by one dimensionful parameter for each mechanism. For Z'-gaugino mediation this parameter is the Z'-gaugino mass $M_{\tilde{Z}'}$, for the anomaly mediation it is the gravitino mass $m_{3/2}$. Comparing 3.4.9 and 3.4.10 we find that they are related by

$$\frac{m_{3/2}}{M_{\tilde{Z}'}} \sim 4\pi. \tag{3.4.14}$$

Such a mild hierarchy between the two mediators can be realized and therefore both, Z'-gaugino and anomaly can be combined to avoid the fine tuning problem for the former and address the negative 'slepton' mass problem of the latter as shown in [41].

The soft scalar terms receive contributions at 1-loop order from the anomaly mediation. Those contributions are given by the RGEs' which are given in [42, 43, 44]. The general expression for the scalar masses is given by [41]

$$m^2 = \frac{m_{3/2}^2}{16\pi^2} \left[\# \, y \, \beta_y - \sum_i 2 \, C_i \, g_i \, \beta_i \right], \tag{3.4.15}$$

where $\#$ is an integer which depends on the specific form of the Yukawa coupling. The constants C_i are

$$C_3 = 4/3, \quad C_2 = 3/4, \quad C_1 = 3\,Y^2/5, \quad C_{z'} = Q^2, \tag{3.4.16}$$

where Y is the hypercharge and Q is the $U(1)'$ charge.

Specifically, the expression for the soft masses of S, H_u, and H_d, at the SUSY breaking scale are,

$$
\begin{aligned}
m_S^2 &= \frac{m_{3/2}^2}{16\pi^2} \left(2\lambda\,\beta_\lambda + 3n_D y_D\,\beta_{y_D} + n_E y_E\,\beta_{y_E} - 2g_{z'}Q_S^2\,\beta_{g_{z'}} \right) \\
m_{H_u}^2 &= \frac{m_{3/2}^2}{16\pi^2} \left(\lambda\,\beta_\lambda + 3y_t\,\beta_{y_t} - \frac{6}{4}g_2\,\beta_{g_2} - \frac{6}{5}Y_{H_u}^2 g_1\,\beta_{g_1} - 2g_{z'}Q_{H_u}^2\,\beta_{g_{z'}} \right) \qquad (3.4.17) \\
m_{H_d}^2 &= \frac{m_{3/2}^2}{16\pi^2} \left(\lambda\,\beta_\lambda + 3y_b\,\beta_{y_b} + y_\tau\,\beta_{y_\tau} - \frac{6}{4}g_2\,\beta_{g_2} - \frac{6}{5}Y_{H_d}^2 g_1\,\beta_{g_1} - 2g_{z'}Q_{H_d}^2\,\beta_{g_{z'}} \right).
\end{aligned}
$$

where β functions are given at 4.1.1, 4.1.2.

The bino, wino, and gluino masses are the MSSM gauginos which are given by [41]

$$
M_1(\Lambda_S) = \frac{\beta_{g_1}}{g_1} m_{3/2}, \quad M_2(\Lambda_S) = \frac{\beta_{g_2}}{g_2} m_{3/2}, \quad M_3(\Lambda_S) = \frac{\beta_{g_3}}{g_3} m_{3/2}. \qquad (3.4.18)
$$

The Z' gaugino mass, $M_{\tilde{Z}'}$, is a free parameter which can be fixed at the scale $M_{\tilde{Z}'}$. Then its value at Λ_S would be given by

$$
M_{\tilde{Z}'}(\Lambda_S) = M_{\tilde{Z}'}(M_{\tilde{Z}'}) \left[1 - \frac{\mathrm{Tr}\,(Q^2)\,g_{z'}^2(\Lambda_s)}{8\pi^2} \ln\left(\frac{\Lambda_S}{M_{\tilde{Z}'}} \right) \right]. \qquad (3.4.19)
$$

Specific illustration point

To get a realistic spectrum we need to have some dimensionful as well as some dimensionless input parameters. Such parameters were chosen for two specific illustration points in [41]. The dimensionless parameters for one of the points are following:

$$U(1)' \text{ gauge coupling (at } \Lambda_S) \quad \text{and charges} \quad : \quad g_{z'} = 0.45 \quad \text{and}$$

$$
Q_{H_u} = -\frac{2}{5}, \quad Q_Q = -\frac{1}{3} \qquad (3.4.20)
$$

$$\text{Superpotential couplings (at } \Lambda_{\mathrm{EW}}) \quad : \quad y_t = 1, y_b = 0.5, y_\tau = 0.294, \lambda = 0.1,$$

$$
y_D = 0.3,\ y_E = 0.5, \qquad (3.4.21)
$$

and the charge assignments to satisfy the anomaly cancellation conditions

	Q	u^c	d^c	L	ν^c	e^c	H_u	H_d	S	D_i	D_i^c	E_i	E_i^c
Q_i	$-\frac{1}{3}$	$\frac{11}{15}$	$-\frac{2}{3}$	$\frac{4}{5}$	$-\frac{2}{5}$	$-\frac{9}{5}$	$-\frac{2}{5}$	1	$-\frac{3}{5}$	$\frac{4}{5}$	$-\frac{1}{5}$	$\frac{9}{5}$	$-\frac{6}{5}$

Table 3.4.1: $U(1)'$ charges used in the model.

We have reproduced the whole mass spectrum of this model as reported in ref. [41], by solving the β-functions for the couplings and the RGEs. The procedure to determine the gaugino masses is described here in detail. Similar method was applied to find other masses.

- We know some couplings at the EW scale which are constant or known and we assume the values of others as shown in Table 3.4.2.

	Known parameters						Assumed parameters					
Parameters	g_1	g_2	g_3	y_τ	y_t	y_b	λ	y_D	y_E	$g_{z'}$	$m_{3/2}$	$M_{\tilde{Z}'}$
Values	0.46	0.65	1.22	0.294	1	0.5	0.1	0.3	0.5	0.45	80 TeV	15 TeV
Scale	EW	EW	EW	EW	EW	EW	EW	EW	EW	Λ_S	Λ_S	$M_{\tilde{Z}'}$

Table 3.4.2: Values of different parameters used to run the RGEs. The values of $\lambda, y_b, y_\tau, m_{3/2}, M_{\tilde{Z}'}$ are considered as free parameters and can be varied for different illustration points.

In choosing the values of gravitino $m_{3/2}$ and $M_{\tilde{Z}'}$ we use the fact that their ratio must maintain the relation 3.4.14

- Use these values as the boundary conditions to simultaneously solve the beta functions for gauge and Yukawa couplings given in appendices.

- Find the values of Yukawa and gauge couplings and beta functions both at EW and SUSY breaking (Λ_S) scales.

- Then use those Λ_S beta function values to find the A terms and gaugino mass terms at Λ_S scale using Eqns 3.5.41, 3.5.40. Since Gauginos are generated at the Λ_S scale, it is important to know their values at this scale.

- Finally solve simultaneously the beta functions for gauge and Yukawa couplings as well as the gamma functions of Gaugino and A terms with the boundary conditions derived in the previous step. Then find the corresponding values at EW scale by running down the RGEs listed in appendix 5.

The one-loop radiative corrections to the scalar masses of H_u, H_d and S are calculated from [46]. We only consider the effects of the stop and top loops as these are the dominant contributions due to the large top Yukawa coupling. The relevant scalar and gaugino mass spectrum for this illustration point are shown in Tables (3.4.3) and (3.4.4). The stop masses are found to be $m_{\tilde{t}_1} = 0.695$ TeV and $m_{\tilde{t}_2} = 3.16$ TeV. The Z' gauge boson mass is found to be $M_{Z'} = 2.78$ TeV.

The other illustration point similarly yields a Z' gauge boson mass, $M_{Z'} = 5.68$ TeV and Higgs mass $m_{h^0} = 0.142$ TeV.

m_{h^0}	$m_{H_1^0}$	$m_{H_2^0}$
0.138 TeV	2.79 TeV	4.78 TeV

Table 3.4.3: Higgs masses

Wino	Gluino	Bino
0.279 TeV	0.399 TeV	1.17 TeV

Table 3.4.4: Gaugino masses

3.5 New results imposing current LHC constraints

All the work described above was done in 2009. After the discovery of the Higgs particle in 2012 [47, 48] the masses presented in Table 3.4.3 are no longer valid and we can now use the Higgs particle mass as an input parameter. LHC provides the

constraints on Z' particle search which includes the dilepton production in Drell-Yan process. There are also constraints on other SUSY particles searches like stop and gluino that can be incorporated in our further analysis of this combined mediation mechanism. In the following subsections we will present our study and results on imposing constraints from Z' and stop searches at the LHC including the Drell-Yan production cross-section of the Z'.

3.5.1   Constraints from Z' gauge boson searches

The Z' gauge bosons are massive and electrically neutral spin-1 particles as predicted by many models. The elementary process for the Z' production is the lowest order Drell-Yan mechanism in which a $q\bar{q}$ pair from hadrons annihilates into a gauge boson and then decays to a l^+l^- pair,

$$q\bar{q} \longrightarrow Z/Z'X \longrightarrow l^+l^-X \tag{3.5.1}$$
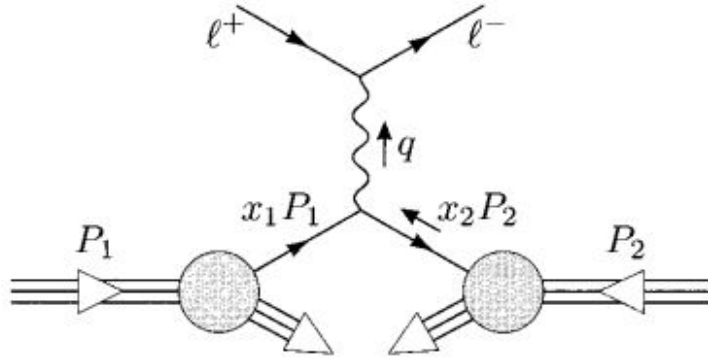

Figure 3.5.1: The Drell-Yan Process: $pp \longrightarrow l^+l^-$ [32]

We derive the amplitude of the Feynman diagram corresponding to this process fol-

lowing [45]. We start with the expression of the amplitude for this process,

$$
i\mathcal{M} = \left[\bar{u}(4)\{-\frac{ig_{Z'}}{2}\gamma^\mu(c_V^f - c_A^f\gamma^5)\}v(3)\right]\left\{\frac{-i(g_{\mu\nu} - \frac{q_\mu q_\nu}{M_{Z'}^2})}{(q^2 - M_{Z'}^2)}\right\}
$$
$$
\left[\bar{v}(2)\{-\frac{ig_{Z'}}{2}\gamma^\nu(c_V^e - c_A^e\gamma^5)\}u(1)\right]
$$
$$
= \left\{\frac{ig_{Z'}^2}{4(q^2 - M_{Z'}^2)}\right\}\left[\bar{u}(4)\gamma^\mu(c_V^f - c_A^f\gamma^5)v(3)\right]\left(g_{\mu\nu} - \frac{q_\mu q_\nu}{M_{Z'}^2}\right)\left[\bar{v}(2)\gamma^\nu(c_V^e - c_A^e\gamma^5)u(1)\right].
$$
$$(3.5.2)$$

Since $\slashed{q} = \slashed{p}_1 + \slashed{p}_2 = \slashed{p}_3 + \slashed{p}_4$ the term containing $q_\mu q_\nu$ contributes nothing, we are left with

$$
\mathcal{M} = \left\{\frac{g_{Z'}^2}{4(q^2 - M_{Z'}^2)}\right\}\left[\bar{u}(4)\gamma^\mu(c_V^f - c_A^f\gamma^5)v(3)\right]\left[\bar{v}(2)\gamma_\mu(c_V^e - c_A^e\gamma^5)u(1)\right]. \qquad (3.5.3)
$$

Thus,

$$
|\mathcal{M}|^2 = \left\{\frac{g_{Z'}^2}{4(q^2 - M_{Z'}^2)}\right\}^2\left[\bar{u}(4)\Gamma_1 v(3)\right]\left[\bar{u}(4)\Gamma_1 v(3)\right]^\dagger\left[\bar{v}(2)\Gamma_2 u(1)\right]\left[\bar{v}(2)\Gamma_2 u(1)\right]^\dagger
$$
$$(3.5.4)$$

with $\Gamma_1 = \gamma^\mu(c_V^f - c_A^f\gamma^5)$ and $\Gamma_2 = \gamma_\mu(c_V^e - c_A^e\gamma^5)$. Averaging over the electron and positron spins s and s' we get,

$$
\frac{1}{4}\left\langle |\mathcal{M}|^2 \right\rangle_{spins} = \left\{\frac{g_{Z'}^2}{8(q^2 - M_{Z'}^2)}\right\}^2 \mathrm{Tr}\left[\slashed{p}_3\gamma^\mu(c_V^f - c_A^f\gamma^5)\slashed{p}_4\gamma^\nu(c_V^f - c_A^f\gamma^5)\right]
$$
$$
\times \mathrm{Tr}\left[\slashed{p}_1\gamma_\alpha(c_V^e - c_A^e\gamma^5)\slashed{p}_2\gamma_\beta(c_V^e - c_A^e\gamma^5)\right]. \quad (3.5.5)
$$

The first trace gives,

$$
\mathrm{Tr}\left[\slashed{p}_3\gamma^\mu(c_V^f - c_A^f\gamma^5)\slashed{p}_4\gamma^\nu(c_V^f - c_A^f\gamma^5)\right] = 4\left\{(c_V^f)^2 + (c_A^f)^2\right\}\left\{(p_3^\mu \cdot p_4^\nu) + (p_3^\nu \cdot p_4^\mu) - \right.
$$
$$
\left. (p_3 \cdot p_4)g^{\mu\nu} - 8iC_V^f C_A^f \epsilon^{\rho\mu\sigma\nu}p_{3\rho}p_{4\sigma}\right\}. \quad (3.5.6)
$$

Similarly for the second trace we get,

$$\text{Tr}\left[\not{p}_1\gamma_\alpha(c_V^e - c_A^e\gamma^5)\not{p}_2\gamma_\beta(c_V^e - c_A^e\gamma^5)\right] = 4\left\{(c_V^e)^2 + (c_A^e)^2\right\}$$
$$\left\{(p_{1\mu}.p_{2\nu}) + (p_{1\nu}.p_{2\mu}) - (p_1.p_2)g_{\mu\nu} - 8iC_V^e C_A^e \epsilon_{\mu\alpha\nu\beta}p_1^\alpha p_2^\beta\right\}. \quad (3.5.7)$$

Thus (3.5.5) becomes

$$\frac{1}{4}\left\langle \mid \mathscr{M} \mid^2 \right\rangle_{spins} = \frac{1}{2}\left\{\frac{g_{Z'}^2}{q^2 - M_{Z'}^2}\right\}^2\left[\left(\left\{(c_V^f)^2 + (c_A^f)^2\right\}\left\{(c_V^e)^2 + (c_A^e)^2\right\}\left\{(p_1.p_3)(p_2.p_4)\right.\right.\right.$$
$$\left.\left.+ (p_1.p_4)(p_2.p_3)\right\}\right) + 4C_V^f C_A^f C_V^e C_A^e\left\{(p_1.p_3)(p_2.p_4) - (p_1.p_4)(p_2.p_3)\right\}\right]. \quad (3.5.8)$$

In the C.M frame the (3.5.8) takes the final form

$$\frac{1}{4}\left\langle \mid \mathscr{M} \mid^2 \right\rangle_{spins} = \left\{\frac{g_{Z'}^2 E^2}{q^2 - M_{Z'}^2}\right\}^2\left[\left\{(c_V^f)^2 + (c_A^f)^2\right\}\left\{(c_V^e)^2 + (c_A^e)^2\right\}(1 + \cos^2\theta)\right.$$
$$\left. - 8C_V^f C_A^f C_V^e C_A^e \cos\theta\right]. \quad (3.5.9)$$

Thus the total cross section is given by

$$\sigma(q\bar{q} \to l^+l^-) = \int d\Omega\left\{\frac{g_{Z'}^2 E}{16\pi\{(2E)^2 - M_{Z'}^2\}}\right\}^2\left[\left\{(c_V^f)^2 + (c_A^f)^2\right\}\left\{(c_V^e)^2 + (c_A^e)^2\right\}\right.$$
$$\left.(1 + \cos^2\theta) - 8C_V^f C_A^f C_V^e C_A^e \cos\theta\right]$$

$$(3.5.10)$$

$$= \frac{1}{3\pi}\left\{\frac{g_{Z'}^2 E}{4\{(2E)^2 - M_{Z'}^2\}}\right\}^2\left(\sum_f Q_f^2\right)\left[\left\{(c_V^f)^2 + (c_A^f)^2\right\}\left\{(c_V^e)^2 + (c_A^e)^2\right\}\right].$$

where the factor 1/3 was introduced in the last line to average over the colors and $\sum_f Q_f^2$ is the square of the quark electric charges.

Narrow Width Approximation (NWA)

At the Z^0 pole the cross-section "blows up" because we treated the Z' particle as a stable particle which is not true. Thus we need to modify the propagator in such a way that effectively treats the produced long-lived state as if it were stable [49],

$$\frac{1}{q^2 - M^2 + i\epsilon} \longrightarrow \frac{1}{q^2 - M^2 + i\Gamma_{Z'}M_{Z'}} \tag{3.5.11}$$

and for Narrow Width Approximation [49] ,

$$\frac{1}{(q^2 - M_{Z'}^2)^2 + \Gamma_{Z'}^2 M_{Z'}^2} \longrightarrow \frac{\pi}{\Gamma_{Z'}M_{Z'}}\delta(q^2 - M_{Z'}^2) \tag{3.5.12}$$

where $\Gamma_{Z'}$ is the total decay width of the Z' particle. If we assume only the SM particles as the final states, then the total decay width is given by [50]

$$\Gamma_{Z'} = \frac{g_{Z'}^2}{48\pi}M_{Z'}\left[9\{(c_V^u)^2+(c_A^u)^2\}+9\{(c_V^d)^2+(c_A^d)^2\}+3\{(c_V^e)^2+(c_A^e)^2\}+3\{(c_V^\nu)^2+(c_A^\nu)^2\}\right].$$
$$\tag{3.5.13}$$

The partial decay for the leptonic decay is given by [51]

$$\Gamma_{Z'\to l^+l^-} = \frac{g_{Z'}^2}{48\pi}\left\{(c_V^e)^2 + (c_A^e)^2\right\}M_{Z'}. \tag{3.5.14}$$

Therefore (3.5.10) can be rewritten as,

$$\sigma(q\bar{q} \to l^+l^-) = \frac{1}{3}\left[\frac{g_{Z'}^2}{48\pi}\left\{(c_V^e)^2 + (c_A^e)^2\right\}M_{Z'}\right]\left(\frac{E^2 g_{Z'}^2}{M_{Z'}}\right)\left\{(c_V^f)^2 + (c_A^f)^2\right\}$$

$$\frac{\pi}{\Gamma_{Z'}M_{Z'}}\delta(q^2 - M_{Z'}^2)$$

$$= BR(Z' \to l^+l^-)\frac{\pi q^2\left\{(c_V^f)^2 + (c_A^f)^2\right\}g_{Z'}^2\delta(q^2 - M_{Z'}^2)}{12M_{Z'}^2},$$

where $q = 2E$, the ratio $1/3$ is the color factor and $BR(Z' \to l^+l^-)$ stands for the

branching ratio of the leptonic decay

$$BR(Z' \to l^+l^-) = \frac{\Gamma_{Z' \to l^+l^-}}{\Gamma_{Z'}}. \tag{3.5.15}$$

Now, if the hard parton-level process involves quark-antiquark scattering at very high energy than the EW scale and then producing a final state Y, the interactions are mainly soft interactions between constituent gluon and quarks. Since the elementary interactions happen very rapidly compared to the internal time-scale of the hadron wavefunctions, the lowest-order prediction should describe the process. Therefore the leading order cross-section should be given by a parton-level formula with the hadron-level cross-section integrated with parton distribution functions. This takes the form [32],

$$\sigma(p(P_1) + p(P_2) \to Y + X) = \sigma(p(P_1) + p(P_2) \to l^+l^- + X) \tag{3.5.16}$$
$$= \int_0^1 dx_1 \int_0^1 dx_2 \sum_f f_f(x_1) f_{\bar{f}}(x_2). \ \sigma(q_f(x_1P) + \bar{q}_f(x_2P) \to Y).$$

where the functions $f_f(x_1)$ are called the *parton distribution functions* (PDFs).

Inserting (**??**) in (3.5.16) we get,

$$\sigma(p(P_1) + p(P_2) \to l^+l^- + X) =$$
$$\int_0^1 dx_1 \int_0^1 dx_2 \sum_f f_f(x_1) f_{\bar{f}}(x_2). \ \sigma(q_f(x_1P) + \bar{q}_f(x_2P) \to l^+l^-) =$$
$$\int_0^1 dx_1 \int_0^1 dx_2 \sum_f f_f(x_1) f_{\bar{f}}(x_2) \frac{\pi q^2 \left\{ (c_V^f)^2 + (c_A^f)^2 \right\} g_{Z'}^2 \delta(q^2 - M_{Z'}^2)}{12 M_{Z'}^2} BR(Z' \to l^+l^-) =$$
$$\int_0^1 dx_1 \int_0^1 dx_2 \sum_f f_f(x_1) f_{\bar{f}}(x_2) \frac{\pi \left\{ (c_V^f)^2 + (c_A^f)^2 \right\} g_{Z'}^2 \delta(\frac{M_{Z'}^2}{s} - x_1 x_2)}{12s} BR(Z' \to l^+l^-).$$

$$\tag{3.5.17}$$

where we have used, the invariant mass $M_{Z'}^2 = q^2 = x_1 x_2 s$ and $\delta(ax) = \frac{1}{|a|}\delta(x)$. Thus finally we get

$$\sigma(p(P_1) + p(P_2) \to l^+ l^- + X) = \frac{\pi}{6s} W_{Z'}(s, M_{Z'}^2) BR(Z' \to l^+ l^-). \tag{3.5.18}$$

where the hadronic structure function is given by

$$W_{Z'}(s, M_{Z'}^2) = g_{Z'}^2 \int_0^1 dx_1 \int_0^1 dx_2 \sum_f f_f(x_1) f_{\bar{f}}(x_2)(Q_f^2 + Q_{f^c}^2)\delta(\frac{M_{Z'}^2}{s} - x_1 x_2), \tag{3.5.19}$$

and the fermionic structure functions are related to the charges by [54]

$$(c_V^f)^2 + (c_A^f)^2 = 2(Q_f^2 + Q_{f^c}^2). \tag{3.5.20}$$

Therefore, the leading order (LO) lepton pair-production cross-section for the Drell-Yan process takes the form

$$\boxed{\sigma(p(P_1) + p(P_2) \to l^+ l^- + X) = \frac{\pi}{6s}\left[c_u w_u(s, M_{Z'}^2) + c_d w_d(s, M_{Z'}^2)\right]}, \tag{3.5.21}$$

where c_u and c_d are given by,

$$c_{u,d} = g_{Z'}^2 \left(Q_{u,d}^2 + Q_{u^c,d^c}^2\right) BR(Z' \to l^+ l^-); \tag{3.5.22}$$

$$w_u = \int_0^1 dx_1 f_u(x_1) \int_0^1 dx_2 f_{\bar{u}}(x_2)\delta(\frac{M_Z^2}{s} - x_1 x_2) \tag{3.5.23}$$

and

$$w_d = \int_0^1 dx_1 f_d(x_1) \int_0^1 dx_2 f_{\bar{d}}(x_2)\delta(\frac{M_Z^2}{s} - x_1 x_2). \tag{3.5.24}$$

The most frequently used formula in the literature for the di-lepton production cross-

section from Z' is given by [50, 52] which takes the form

$$\sigma(p\bar{p} \to Z'X \to l^+l^-X) = \frac{\pi}{48s}\left[c_u w_u(s, M_{Z'}^2) + c_d w_d(s, M_{Z'}^2)\right]. \qquad (3.5.25)$$

Comparing (3.5.25) with (3.5.21) we find that the difference between two expressions is a factor of 8.

Usually the experimental constraints on Z' production cross-section, presented in c_d - c_u plane [53], refer to eqn. (3.5.25). The purpose of this long and detailed calculation to derive the eqn. (3.5.21) is to understand the the constraints on Z' mass presented by experiments. Therefore we want to know if our understanding of the constraints on Z' mass can be affected by the factor 8 that we found in our study. We shall discuss that in the following subsections.

3.5.2 c_d - c_u plane parameterization

From (3.5.21) it is found that the parameters c_u and c_d contain all the model dependence of the cross-section. Knowing $g_{z'}, c_u$ and c_d and assuming that Z' decays only to the SM particles, the experimental bound on $pp(\bar{p}) \to Z' \to \ell^+\ell^-$ cross sections from the Lagrangian parameters can be estimated. These bounds can be compared with theoretically predicted values. We can calculate these parameters systematically in the following way:

Calculation of vector and axial couplings

The vector and axial couplings, c_V^f and c_A^f respectively are related to the charge assignments as [54]

$$c_V^f = Q_f - Q_{f^c}, \qquad c_A^f = Q_f + Q_{f^c}. \qquad (3.5.26)$$

So, for all benchmark models these couplings can be calculated directly from their

respective charge assignments.

Calculation of the branching ratio

Once the couplings are calculated they can be used to calculate the branching ratio from equations (3.5.13), (3.5.14) and (3.5.15).

Calculation of the PDFs

The quantities w_u and w_d are evaluated from MSTW08 [55] set of Parton Distribution Functions(PDFs). To access these PDF sets the mathematica pacage of MSTW08 PDFs codes and Leading Order (LO) grids have been used. The factorization scale used for these calculation is $q = M_{Z'}$.

Creating c_d - c_u plane from experimental data

Using the cross-section formula with the correct factor, eqn. (3.5.21), it is found that for a given Z' mass, the experimental cross-section data and the charge assignment of a model help us to relate c_u and c_d linearly [50],

$$c_u = a - bc_d \tag{3.5.27}$$

where a, b are given by

$$a = \frac{6s}{\pi} \frac{\sigma_{\ell^+\ell^-}^{exp}}{w_u}, \qquad b = \frac{w_d}{w_u}. \tag{3.5.28}$$

We used the 95% Confidence Label (C.L) data on the upper bound of the cross-section, Z' dacaying to dilepton, from the D0 collaboration [56]. Using those data we were able to transform the experimental information to the c_d - c_u plane and produce the plot (3.5.2 (a)) similar to those shown in [50].

Higher-order corrections

The higher-order corrections are given in the form of K-factors for Next to Leading Order (NLO) or Next to Next to Leading Order (NNLO). These K-factors are defined as [50]

$$K_i = \frac{\sigma(pp(\bar{p}) \to Z')_i}{\sigma(pp(\bar{p}) \to Z')_0}, \tag{3.5.29}$$

where the index $i = 1, 2$ corresponds to NLO and NNLO K-factors, respectively.

For our analysis purpose the NNLO K-factor were also included into our calculations and the modified Drell-Yan cross-section becomes [50]

$$\sigma_{l^+l^+}^{NNLO} \simeq K_{NNLO}^{PDF}\sigma_{l^+l^+}^{LO}, \tag{3.5.30}$$

where the $\sigma_{l^+l^+}^{LO}$ is given by the (3.5.21).

The detailed analysis and the results obtained will be shown here.

Comparison of results in $c_d - c_u$ plane

The data set was used from the D0 collaboration [56] where $\sqrt{s} = 1.96$ TeV and the cross-section values were reported from $175 - 1100$ GeV. We have plotted from 600 GeV to 1100 GeV in c_d - c_u plane following the steps explained in Section 3.5.2. This is shown in the Figure 3.5.2(a) here. The plot is similar to the FIG 7 in [50] which we have presented here in the Figure 3.5.2(b) for comparison purpose. In Figure 3.5.2, each contour corresponds to a particular Z' gauge boson mass value.
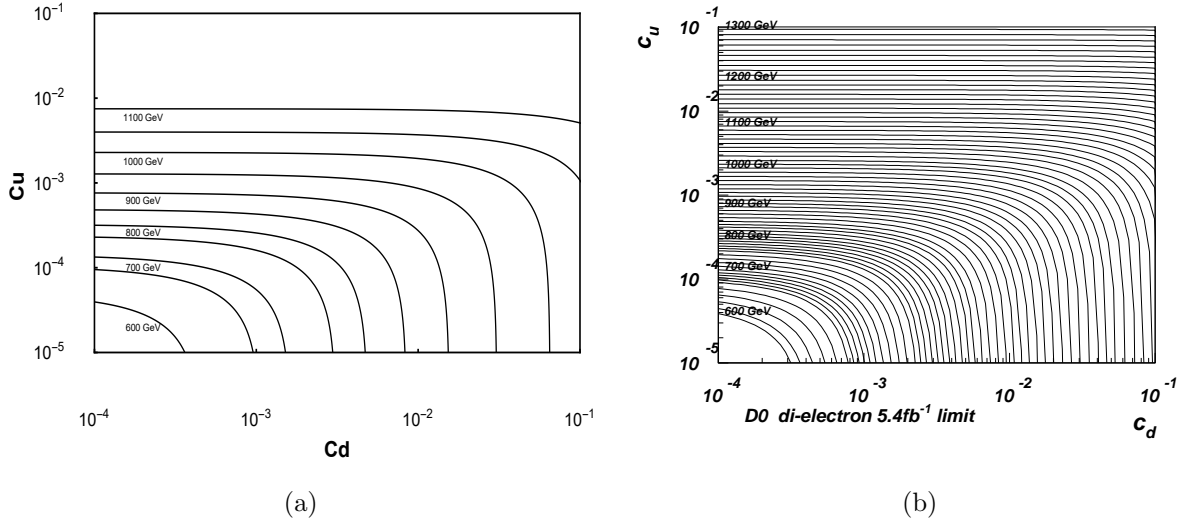
Figure 3.5.2: *Left panel : The contours are created using cross-section data taken from [56] and then plugging in 3.5.31. Right panel : FIG 7 plot also using the same data set as shown in [50].*

To generate the contours on the c_d - c_u plane equations (3.5.27) and (3.5.28) were used. According to (3.5.28), a can be different depending on what expression ((3.5.21) or (3.5.25)) is chosen to work with and/or whether we choose to include the K factors or not. Therefore when the data set was plotted in the c_d - c_u plane, there are four possibilities which must be taken into account. The reason being the size of the K-factor might mitigate the difference (the factor of 8) between the expressions and that can be verified by considering all those possible combinations. 700 GeV data set was used as the reference for our analysis. For a fixed energy value and fixed PDF set, these possibilities are:

1. use (3.5.21),

$$\sigma(p(P_1) + p(P_2) \rightarrow l^+l^- + X) = \frac{\pi}{6s}\left[c_u w_u(s, M_{Z'}^2) + c_d w_d(s, M_{Z'}^2)\right],$$

2. use (3.5.25),

$$\sigma(p\bar{p} \to Z'X \to l^+l^-X) = \frac{\pi}{48s}\left[c_u w_u(s, M_{Z'}^2) + c_d w_d(s, M_{Z'}^2)\right],$$

3. use (3.5.30) with $\sigma_{l^+l^+}^{LO}$ given by (3.5.21)

$$\sigma_{l^+l^+}^{NNLO}(p(P_1) + p(P_2) \to l^+l^- + X) \simeq K_{NNLO}^{PDF} \times \frac{\pi}{6s}\left[c_u w_u(s, M_{Z'}^2) + c_d w_d(s, M_{Z'}^2)\right],$$

(3.5.31)

and

4. use (3.5.30) with $\sigma_{l^+l^+}^{LO}$ given by (3.5.25)

$$\sigma_{l^+l^+}^{NNLO}(p(P_1) + p(P_2) \to l^+l^- + X) \simeq K_{NNLO}^{PDF} \times \frac{\pi}{48s}\left[c_u w_u(s, M_{Z'}^2) + c_d w_d(s, M_{Z'}^2)\right].$$

(3.5.32)

.

The K_{NNLO} factors vary from 1.22-1.29 [56] for the energy range chosen here. It is interesting to notice the fact that all contours of the Figure 3.5.2(b) are claimed in [50] to be derived by using (3.5.25) with the K-factor and wrong factor of 48 in front. That is equivalent to the possibility 4 as described above but actually the similar contours can be derived by using the possibility 3 as shown in Figure 3.5.2(a).

Benchmark models	Z' mass limits (GeV) using (3.5.21)	Z' mass limits (GeV) using (3.5.25)
$U(1)_{GSM}$	1020	800
$U(1)_{\psi}$	915	650
$U(1)_{\chi}$	915	650

Table 3.5.1: *Z' mass lower limits of different benchmark models, using different cross-section formula.*

For any theoretical model the c_d and c_u values can be obtained directly from the charge assignment. Therefore the Z' mass limit can be obtained easily by plotting those values in

the c_d-c_u plane as shown in Figure 3.5.3. In both panels of Figure 3.5.3, 'Blue dot', 'Orange box' and 'Red diamond' represent $U(1)'_{SSM}$, $U(1)'_\chi$ and $U(1)'_\psi$ models respectively. Table 3.5.1 shows the lower bounds on Z' mass obtained from $c_d - c_u$ parameterization for different benchmark models. The second column of Table 3.5.1 gives the mass limits reported in [50] for these benchmark models. But the values reported there are actually obtained if (3.5.21) is used to create the $c_d - c_u$ contours. This is shown in Figure 3.5.3(a). On the contrary the formula used in [50] to produce the $c_d - c_u$ contours is (3.5.25). According to that the corresponding contours should look like as shown in the Figure 3.5.3(b) and the corresponding Z' mass limits should be as reported in the third column in Table 3.5.1.
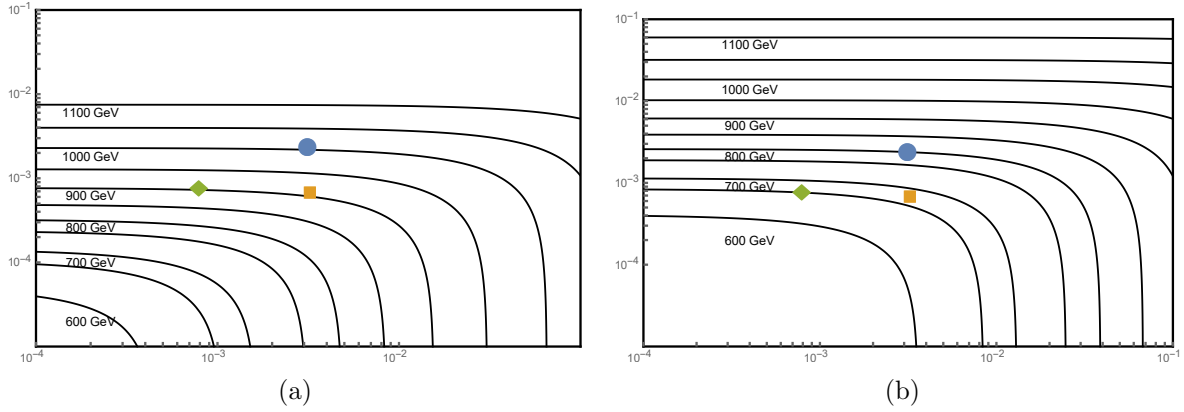
Figure 3.5.3: *Left panel : The Z′ mass limits for the benchmark models reported in [50] actually obtained by using* (3.5.21). *Right panel :The actual Z′ mass limits should be obtained for the benchmark models using* (3.5.25) *as described in [50]. In both panels 'Blue dot', 'Orange box' and 'Red diamond' represent* $U(1)'_{SSM}$, $U(1)'_\chi$ *and* $U(1)'_\psi$ *models respectively.*

3.5.3   Summary of $c_u - c_d$ parameterization

From the above discussion it can be concluded that the formula (eqn.(3.5.25)) which is claimed to be applied to obtain the results in ref.[50] and the actual results are not consistent with each other. The results that we have calculated are fine in the sense

that they actually do not use the eqn.(3.5.25) to get their results, rather they use some computational methods which somehow take care of the concerning factor of 8.

Since the contour in the $c_d - c_u$ plane represents the exclusion limit on the Z' mass, it is very important to get the correct contour through correct formula. It is shown in Table 3.5.1 that if different formulas are used to obtain the cross-section, the mass limits also change. Therefore the difference of the factor of 8 between the two above mentioned equations (3.5.21 & 3.5.25) is significant and need to be addressed more carefully.

3.5.4 Using LHC constraints from stop and gluino search

To impose the LHC constraints on this model we need to know which parameters are important in determining the whole mass spectrum.

Fermion and sfermion masses

The fermions masses are given by

$$m_{f_i} = y_i \langle \phi_i \rangle. \tag{3.5.33}$$

where y_i have non-zero values only for the third generation of fermions, and the exotics D and E. Also, $\phi_t = H_u^0$, $\phi_{b,\tau} = H_d^0$, and $\phi_{D,E} = S$. All the vevs are assumed to be real.

The sfermion mass matrices can be written in a compact form as [41]

$$m_{\tilde{f}_i}^2 = \begin{pmatrix} m_{\tilde{f}_{i1}}^2 + y_i^2 \langle \phi_i \rangle^2 + \Delta_{\tilde{f}_{i1}} & \pm\lambda\, y_i \langle S \rangle \langle H_u^0 \rangle \langle H_d^0 \rangle / \langle \phi_i \rangle \mp A_{y_i}^* \langle \phi_i \rangle \\ \pm\lambda\, y_i \langle S \rangle \langle H_u^0 \rangle \langle H_d^0 \rangle / \langle \phi_i \rangle \mp A_{y_i} \langle \phi_i \rangle & m_{\tilde{f}_{i2}}^2 + y_i^2 \langle \phi_i \rangle^2 + \Delta_{\tilde{f}_{i2}} \end{pmatrix},$$

(3.5.34)

where the upper signs are for the $\tilde{t}$ and the lower are for the $\tilde{b}$, $\tilde{\tau}$, $\tilde{D}$, and $\tilde{E}$. In the last equation y_i and A_{y_i} are non-zero only for third generation sfermions and the scalar

exotics. The notation for the soft masses is such that for squarks and sleptons $m^2_{\tilde{f}_{i1}}$ is the $SU(2)_L$ doublet soft mass and $m^2_{\tilde{f}_{i2}}$ is the right-handed soft mass. For the exotics $m^2_{\tilde{f}_{D1}} = m^2_{\tilde{D}}$, $m^2_{\tilde{f}_{E1}} = m^2_{\tilde{E}}$, $m^2_{\tilde{f}_{D2}} = m^2_{\tilde{D}^c}$, $m^2_{\tilde{f}_{E2}} = m^2_{\tilde{E}^c}$. Also

$$
\begin{aligned}
\Delta_{\tilde{f}_{i1}} &= \frac{1}{2}\left(g_2^2 T^3_{i1} - \frac{3}{5}g_1^2 Y_{i1}\right)\left(\langle H_d^0\rangle^2 - \langle H_u^0\rangle^2\right) + g_{Z'}^2 Q_{i1}\left(Q_S\langle S\rangle^2 + Q_{H_u}\langle H_u^0\rangle^2 + Q_{H_d}\langle H_d^0\rangle^2\right) \\
\Delta_{\tilde{f}_{i2}} &= \frac{1}{2}\left(g_2^2 T^3_{i2} - \frac{3}{5}g_1^2 Y_{i2}\right)\left(\langle H_d^0\rangle^2 - \langle H_u^0\rangle^2\right) + g_{Z'}^2 Q_{i2}\left(Q_S\langle S\rangle^2 + Q_{H_u}\langle H_u^0\rangle^2 + Q_{H_d}\langle H_d^0\rangle^2\right),
\end{aligned}
$$

$$(3.5.35)$$

where T^3 and Y are the third component of the weak isospin and the weak hypercharge, respectively and $Q_{i1,i2,S \text{ etc}}$ are the charge assignment of the model given in [41].

Therefore for stop particles, 3.5.35 gives

$$
\begin{aligned}
\Delta_{\tilde{t}_1} &= \frac{1}{2}\left(g_2^2 T^3_Q - \frac{3}{5}g_1^2 Y_Q\right)\left(v_d^2 - v_u^2\right) + g_{Z'}^2 Q_Q\left(Q_S s^2 + Q_{H_u}v_u^2 + Q_{H_d}v_d^2\right) \\
\Delta_{\tilde{t}_2} &= \frac{1}{2}\left(g_2^2 T^3_{t^c} - \frac{3}{5}g_1^2 Y_{t^c}\right)\left(v_d^2 - v_u^2\right) + g_{Z'}^2 Q_{t^c}\left(Q_S s^2 + Q_{H_u}v_u^2 + Q_{H_d}v_d^2\right).
\end{aligned}
$$

$$(3.5.36)$$

Explicitly, using 3.5.36 the stop mass matrix is given by

$$
\begin{aligned}
m^2_{\tilde{t}_i} &= \begin{pmatrix} m^2_{\tilde{t}_1} + y_i^2\langle\phi_i\rangle^2 + \Delta_{\tilde{t}_1} & \lambda\, y_t\langle S\rangle\langle H_u^0\rangle\langle H_d^0\rangle/\langle\phi_i\rangle - A^*_{y_i}\langle\phi_i\rangle \\ \\ \lambda\, y_t\langle S\rangle\langle H_u^0\rangle\langle H_d^0\rangle/\langle\phi_i\rangle - A_{y_i}\langle\phi_i\rangle & m^2_{\tilde{t}_2} + y_i^2\langle\phi_i\rangle^2 + \Delta_{\tilde{t}_2} \end{pmatrix} \\ \\
&= \begin{pmatrix} m^2_{\tilde{Q}_3} + y_t^2 v_u^2 + \Delta_{\tilde{t}_1} & \lambda\, y_t s v_d - A^*_{y_t} v_u \\ \\ \lambda\, y_t s v_d - A_{y_t} v_u & m^2_{\tilde{t}^c} + y_t^2 v_u^2 + \Delta_{\tilde{t}_2} \end{pmatrix}
\end{aligned}
$$

(3.5.37)

where $m^2_{\tilde{Q}_3}$ and $m^2_{\tilde{t}^c}$ are third generation squark mass-squared.

Therefore the physical stop masses are given by [46]

$$m^2_{\tilde{t}_{1,2}} = \frac{1}{2}\text{tr}\mathcal{M}_{\tilde{t}} \mp \frac{1}{2}\sqrt{(\text{tr}\mathcal{M}_{\tilde{t}})^2 - 4\det\mathcal{M}_{\tilde{t}}} \qquad (3.5.38)$$

where $\mathcal{M}_{\tilde{t}}$ is equivalent to 3.5.37.

3.5.5 Using constraints on stop mass

From 3.5.38,3.5.37 and 3.5.36 we find that there are seven independent parameters which determine the physical stop masses, namely

$$m^2_{\tilde{Q}_3}, m^2_{\tilde{t}^c}, g_{Z'}, \tan\beta, s, A_{yt} \text{ and } \lambda. \qquad (3.5.39)$$

where $\tan\beta$ is defined as v_u/v_d. Using the current LHC constraints obtained from stop mass searches we can try to put some bounds on these parameters.

Parameter scans

Most recent searches for stop particles in different methods at the LHC sets a lower limit from $90\text{ GeV} - 950\text{ GeV}$ [57].

Therefore we take a conservative limit to set the lower limit of the stop masses to be 2 TeV for our case. We chose 10 TeV to be the upper limit. To generate this stop mass we perform some scans over the allowed parameter spaces. We evaluated more than 227000 points in the available parameter space for these scans. It is a common practice to fix $m_{\tilde{t}^c}$ and $m_{\tilde{Q}_3}$, the up-type squarks and doublet-type squarks respectively, at 1 TeV. But to be more generic we also decided to vary those parameters. The ranges, the corresponding step sizes and the limits for those parameters obtained from the scan are shown in Table 3.5.2.

Parameters	$g_{z'}$	$\tan\beta$	A_t(TeV)	λ	$m_{\tilde{Q}_3}$(TeV)	$m_{\tilde{t}^c}$(TeV)	s(TeV)
Scanned range	0.2 - 0.8	1 - 121	0.01 - 30.01	.01 - 1.25	0.01 - 24.01	0.01 - 24.01	$0.01 - 24.01$
Step size	0.01	2	0.5	$10^{0.035}$	0.4	0.4	0.4
Lower limit	0.25	9	0.01	0.01	1.61	2.01	1.61
Upper limit	0.8	49	20.51	0.27	9.61	24.01	9.61

Table 3.5.2: Parameter ranges used for the scan and their limits obtained from the scan

3.5.6   Using constraints on gluino mass

The method to generate the gaugino masses is described in detail in Section 3.4.5.

Gaugino mass terms and relevant parameters

The gaugino and the scalar masses are assumed to be generated at the SUSY breaking scale from the anomaly mediation. We took the general expression for the gaugino and A terms from [58]

$$M_\lambda = -\frac{g^2}{2}\frac{dg^{-2}}{d\ln\mu}m_{3/2} = \frac{\beta_g}{g}m_{3/2} \tag{3.5.40}$$

$$A_y = \frac{1}{2}\sum_i \frac{d\ln Z_{Q_i}}{d\ln\mu}m_{3/2} = -\beta_y m_{3/2}, \tag{3.5.41}$$

where $\gamma \equiv d\ln Z/d\ln\mu$, $\beta_g \equiv dg/d\ln\mu$, $\beta_y \equiv dy/d\ln\mu$, and A_y is defined as in $\mathcal{L} = -A_y\,\phi_1\,\phi_2\,\phi_3$ +h.c.. At one loop

$$\gamma_j^i = -\frac{1}{16\pi^2}\left[y^{imn}y^*_{jmn} - 4g_a^2 C_a(i)\delta_j^i\right]. \tag{3.5.42}$$

To determine the boundary conditions, we need the beta functions for the gauge and Yukawa couplings which are given in [41]. These boundary values then used to obtain the parameters at the EW scale.

The MSSM gaugino masses at the SUSY breaking scale are given by 3.4.18. The Z' gaugino mass, $M_{\tilde{Z}'}$, is a free parameter. If we fix it at the scale $M_{\tilde{Z}'}$, its value at Λ_S would be given by eqn. 3.4.19.

To get the physical masses we then need to run down to the EW scale using RGEs given in [41]. Since the gaugino mass parameters contribute strongly to other soft mass parameters we also need to run their corresponding RGEs.

From the parameters mentioned in 3.5.39, only few parameters are necessary for determining the gaugino masses. The values of λ, and $g_{z'}$ are needed as the boundary conditions at EW scale to determine the Yukawa and gauge couplings and corresponding beta functions at Λ_S scale. These beta functions are necessary to generate the corresponding A terms and gaugino masses at Λ_S scale. Therefore in this section we plan only to study the significance of λ, $g_{z'}$ and A_{yt} parameters in detail for our analysis.

Using allowed λ values from stop mass parameters scan

From the parameters scan we performed, for stop masses to be in the experimental allowed region, we found there are 42 different values of λ with the range shown in Table 3.5.2. We first take these different λ values at EW scale and run the RGEs upto Λ_S scale. Now Eqns. 3.5.40 and 3.5.41 tell us that we need to evaluate those beta functions for Yukawa and gauge couplings at Λ_S scale for A terms and gaugino mass calculations. The SUSY breaking scale, Λ_S, used for the analysis is 5×10^6 TeV.

Results of this analysis

If we follow the general procedures as explained in the Section 3.4.5, to evaluate the gaugino masses, we find that at Λ_S scale only the values of the Yukawa couplings change, but not the values of gauge couplings. The reason of this behavior lies in the RG Equations for these couplings. Looking at those RGEs in 4.1.1 we find that the gauge coupling RGEs are suppressed by an additional factor of $\frac{1}{16\pi^2}$. Therefore actually the

change in the gauge couplings occur at the order of 10^{-8} or beyond and thus negligible. But the corresponding beta-functions for Yukawa couplings change significantly due to their one-loop structure.

3.6 Conclusion and outlook

From the current LHC data we have imposed the constraints on the Z'-boson mass. Since the Z' mass, $M_{Z'} \approx g_{z'} Q_S \langle S \rangle$ and $c_{u,d} \propto g_{z'}^2$, it is extremely important to choose suitable $g_{z'}$ and $\langle S \rangle$ to be in the experimentally allowed region.

From the parameters scan we performed, for stop and gluino masses, we discussed only the implication of few parameters with their allowed ranges. We plan to explore other relevant parameters such as $g_{Z'}$ and A_{yt} and their allowed spaces as our future work.

We also plan to use the observed Higgs mass (125 GeV) as an input to scan the parameter space, update the whole mass spectrum [59].

CHAPTER 4: BOUNDARY CONDITIONS AND OTHER PARAMETERS

To determine the gaugino masses we need both the β-functions of gauge and Yukawa couplings which are given below

4.1 Gauge and Yukawa β functions

The gauge coupling β functions are

$$
\begin{aligned}
\beta_{g_1} &= \frac{g_1^3}{16\pi^2}\left\{\frac{51}{5} + \frac{1}{16\pi^2}\left[24g_3^2 + \frac{27}{5}g_2^2 + \frac{351}{25}g_1^2 + g_{z'}^2\frac{12}{5}\mathrm{Tr}\left(Y^2Q^2\right)\right.\right. \\
&\qquad\left.\left. -\frac{26}{5}y_t^2 - \frac{14}{5}y_b^2 - \frac{18}{5}y_\tau^2 - \frac{6}{5}\lambda^2 - \frac{12}{5}y_D^2 - \frac{24}{5}y_E^2\right]\right\} \\
\beta_{g_2} &= \frac{g_2^3}{16\pi^2}\left\{1 + \frac{1}{16\pi^2}\left[24g_3^2 + 25g_2^2 + \frac{9}{5}g_1^2 + 2g_{z'}^2(Q_{H_d}^2 + Q_{H_u}^2 + 3(Q_L^2 + 3Q_Q^2))\right.\right. \\
&\qquad\left.\left. -6y_t^2 - 6y_d^2 - 2y_\tau^2 - 2\lambda^2\right]\right\} \\
\beta_{g_3} &= \frac{g_3^3}{(16\pi^2)^2}\left[48g_3^2 + 9g_2^2 + 3g_1^2 + 6g_{z'}^2(Q_D^2 + Q_{D^c}^2 + 2Q_Q^2 + Q_{u^c}^2 + Q_{d^c}^2) - \right. \\
&\qquad\left. 4y_t^2 - 4y_b^2 - 6y_D^2\right] \\
\beta_{g_{Z'}} &= \frac{g_{Z'}^3}{16\pi^2}\left\{\mathrm{Tr}\left(Q^2\right) + \frac{1}{16\pi^2}\left[4g_{z'}^2\mathrm{Tr}\left(Q^4\right) + g_1^2\frac{12}{5}\mathrm{Tr}\left(Y^2Q^2\right)\right.\right. \\
&\qquad +6g_2^2(Q_{H_d}^2 + Q_{H_u}^2 + 3(Q_L^2 + 3Q_Q^2)) + 48g_3^2(Q_D^2 + Q_{D^c}^2 + 2Q_Q^2 + Q_{u^c}^2 + Q_{d^c}^2) - \\
&\qquad -12(Q_{u^c}^2 + Q_Q^2 + Q_{H_u}^2)y_t^2 - 12(Q_{d^c}^2 + Q_Q^2 + Q_{H_d}^2)y_b^2 - 4(Q_{e^c}^2 + Q_L^2 + Q_{H_d}^2)y_e^2 \\
&\qquad\left.\left. -18(Q_{D^c}^2 + Q_D^2 + Q_S^2)y_D^2 - 4(Q_{E^c}^2 + Q_E^2 + Q_S^2)y_E^2 - 4(Q_{H_u}^2 + Q_{H_d}^2 + Q_S^2)\lambda^2\right]\right\}.
\end{aligned}
$$

$$(4.1.1)$$

The relevant β functions for the Yukawa couplings are

$$
\begin{aligned}
\beta_{y_t} &= \frac{y_t}{16\pi^2}\left[\lambda^2 + 6y_t^2 + y_b^2 - \frac{16}{3}g_3^2 - 3g_2^2 - \frac{13}{15}g_1^2 - 2g_{z'}^2(Q_{H_u}^2 + Q_Q^2 + Q_{u^c}^2)\right] \\
\beta_{y_b} &= \frac{y_b}{16\pi^2}\left[\lambda^2 + 6y_b^2 + y_t^2 + y_e^2 - \frac{16}{3}g_3^2 - 3g_2^2 - \frac{7}{15}g_1^2 - 2g_{z'}^2(Q_{H_d}^2 + Q_Q^2 + Q_{d^c}^2)\right] \\
\beta_{y_\tau} &= \frac{y_\tau}{16\pi^2}\left[\lambda^2 + 3y_b^2 + 4y_\tau^2 - 3g_2^2 - \frac{9}{5}g_1^2 - 2g_{z'}^2(Q_{H_d}^2 + Q_L^2 + Q_{e^c}^2)\right] \\
\beta_\lambda &= \frac{\lambda}{16\pi^2}\left[4\lambda^2 + 3y_t^2 + 3y_b^2 + y_\tau^2 + 3n_D\, y_D^2 + n_E\, y_E^2 - 3g_2^2 - \frac{3}{5}g_1^2 - \right. \tag{4.1.2} \\
&\qquad \left. 2g_{z'}^2\left(Q_S^2 + Q_{H_u}^2 + Q_{H_d}^2\right)\right] \\
\beta_{y_D} &= \frac{y_D}{16\pi^2}\left[2\lambda^2 + (3n_D + 2)y_D^2 + n_E y_E^2 - \frac{16}{3}g_3^2 - \frac{6}{5}g_1^2(Y_D^2 + Y_{D^c}^2) - \right. \tag{4.1.3} \\
&\qquad \left. 2g_{z'}^2(Q_S^2 + Q_D^2 + Q_{D^c}^2)\right] \\
\beta_{y_E} &= \frac{y_E}{16\pi^2}\left[2\lambda^2 + 3n_D y_D^2 + (n_E + 2)y_E^2 - \frac{6}{5}g_1^2(Y_E^2 + Y_{E^c}^2) - 2g_{z'}^2(Q_S^2 + Q_E^2 + Q_{E^c}^2)\right]. \\
&\tag{4.1.4}
\end{aligned}
$$

We have set all the SM Yukawas, apart from y_t, y_b, and y_τ, to zero.

4.2 Gaugino masses

The MSSM gaugino masses are

$$
M_3(\Lambda_S) = \frac{\beta_{g_3}}{g_3}\, m_{3/2}, \quad M_2(\Lambda_S) = \frac{\beta_{g_2}}{g_2}\, m_{3/2}, \quad M_1(\Lambda_S) = \frac{\beta_{g_1}}{g_1}\, m_{3/2}. \tag{4.2.1}
$$

The Z' gaugino mass, $M_{\tilde{Z}'}$, is a free parameter. If we fix it at the scale $M_{\tilde{Z}'}$, its value at Λ_S would be

$$
M_{\tilde{Z}'}(\Lambda_S) = M_{\tilde{Z}'}(M_{\tilde{Z}'})\left[1 - \frac{\mathrm{Tr}\,(Q^2)\, g_{z'}^2(\Lambda_s)}{8\pi^2}\ln\left(\frac{\Lambda_S}{M_{\tilde{Z}'}}\right)\right]. \tag{4.2.2}
$$

4.3   Scalar masses

The general expression for the scalar masses is schematically

$$m^2 = \frac{m_{3/2}^2}{16\pi^2} \left[\# \, y \, \beta_y - \sum_i 2 \, C_i \, g_i \, \beta_i \right], \tag{4.3.1}$$

where $\#$ is an integer which depends on the specific form of the Yukawa coupling. The constants C_i are

$$C_3 = 4/3, \quad C_2 = 3/4, \quad C_1 = 3 \, Y^2/5, \quad C_{z'} = Q^2, \tag{4.3.2}$$

where Y is the hypercharge and Q is the $U(1)'$ charge.

The expression for the soft masses at the SUSY breaking scale are, for S, H_u, and H_d,

$$m_S^2 = \frac{m_{3/2}^2}{16\pi^2} \left(2\lambda \, \beta_\lambda + 3 n_D y_D \, \beta_{y_D} + n_E y_E \, \beta_{y_E} - 2 g_{z'} Q_S^2 \, \beta_{g_{z'}} \right)$$

$$m_{H_u}^2 = \frac{m_{3/2}^2}{16\pi^2} \left(\lambda \, \beta_\lambda + 3 y_t \, \beta_{y_t} - \frac{6}{4} g_2 \, \beta_{g_2} - \frac{6}{5} Y_{H_u}^2 g_1 \, \beta_{g_1} - 2 g_{z'} Q_{H_u}^2 \, \beta_{g_{z'}} \right)$$

$$m_{H_d}^2 = \frac{m_{3/2}^2}{16\pi^2} \left(\lambda \, \beta_\lambda + 3 y_b \, \beta_{y_b} + y_\tau \, \beta_{y_\tau} - \frac{6}{4} g_2 \, \beta_{g_2} - \frac{6}{5} Y_{H_d}^2 g_1 \, \beta_{g_1} - 2 g_{z'} Q_{H_d}^2 \, \beta_{g_{z'}} \right) \tag{4.3.3}$$

for the scalar exotics,

$$m_{\tilde{D}}^2 = \frac{m_{3/2}^2}{16\pi^2} \left(y_D \, \beta_{y_D} - \frac{8}{3} g_3 \, \beta_{g_3} - \frac{6}{5} Y_D^2 g_1 \, \beta_{g_1} - 2 g_{z'} Q_D^2 \, \beta_{g_{z'}} \right)$$

$$m_{\tilde{D}^c}^2 = \frac{m_{3/2}^2}{16\pi^2} \left(y_D \, \beta_{y_D} - \frac{8}{3} g_3 \, \beta_{g_3} - \frac{6}{5} Y_{D^c}^2 g_1 \, \beta_{g_1} - 2 g_{z'} Q_{D^c}^2 \, \beta_{g_{z'}} \right)$$

$$m_{\tilde{E}}^2 = \frac{m_{3/2}^2}{16\pi^2} \left(y_E \, \beta_{y_E} - \frac{6}{5} Y_E^2 g_1 \, \beta_{g_1} - 2 g_{z'} Q_E^2 \, \beta_{g_{z'}} \right)$$

$$m_{\tilde{E}^c}^2 = \frac{m_{3/2}^2}{16\pi^2} \left(y_E \, \beta_{y_E} - \frac{6}{5} Y_{E^c}^2 g_1 \, \beta_{g_1} - 2 g_{z'} Q_{E^c}^2 \, \beta_{g_{z'}} \right); \tag{4.3.4}$$

for the third generation squarks

$$
\begin{aligned}
m_{\tilde{Q}_3}^2 &= \frac{m_{3/2}^2}{16\pi^2}\left(y_t\,\beta_{y_t} + y_b\,\beta_{y_b} - \frac{8}{3}g_3\,\beta_{g_3} - \frac{6}{4}g_2\,\beta_{g_2} - \frac{6}{5}Y_Q^2 g_1\,\beta_{g_1} - 2g_{z'}Q_Q^2\,\beta_{g_{z'}} \right) \\
m_{\tilde{t}^c}^2 &= \frac{m_{3/2}^2}{16\pi^2}\left(2y_t\,\beta_{y_t} - \frac{8}{3}g_3\,\beta_{g_3} - \frac{6}{5}Y_{u^c}^2 g_1\,\beta_{g_1} - 2g_{z'}Q_{u^c}^2\,\beta_{g_{z'}} \right) \\
m_{\tilde{b}^c}^2 &= \frac{m_{3/2}^2}{16\pi^2}\left(2y_b\,\beta_{y_b} - \frac{8}{3}g_3\,\beta_{g_3} - \frac{6}{5}Y_{d^c}^2 g_1\,\beta_{g_1} - 2g_{z'}Q_{d^c}^2\,\beta_{g_{z'}} \right) ;
\end{aligned}
\tag{4.3.5}
$$

for the first two generations of squarks,

$$
\begin{aligned}
m_{\tilde{Q}_i}^2 &= \frac{m_{3/2}^2}{16\pi^2}\left(-\frac{8}{3}g_3\,\beta_{g_3} - \frac{6}{4}g_2\,\beta_{g_2} - \frac{6}{5}Y_Q^2 g_1\,\beta_{g_1} - 2g_{z'}Q_Q^2\,\beta_{g_{z'}} \right) \\
m_{\tilde{u}_i^c}^2 &= \frac{m_{3/2}^2}{16\pi^2}\left(-\frac{8}{3}g_3\,\beta_{g_3} - \frac{6}{5}Y_{u^c}^2 g_1\,\beta_{g_1} - 2g_{z'}Q_{u^c}^2\,\beta_{g_{z'}} \right) \\
m_{\tilde{d}_i^c}^2 &= \frac{m_{3/2}^2}{16\pi^2}\left(-\frac{8}{3}g_3\,\beta_{g_3} - \frac{6}{5}Y_{d^c}^2 g_1\,\beta_{g_1} - 2g_{z'}Q_{d^c}^2\,\beta_{g_{z'}} \right) ;
\end{aligned}
\tag{4.3.6}
$$

for the third generation of charged sleptons,

$$
\begin{aligned}
m_{\tilde{L}_3}^2 &= \frac{m_{3/2}^2}{16\pi^2}\left(y_\tau\,\beta_{y_\tau} - \frac{6}{4}g_2\,\beta_{g_2} - \frac{6}{5}Y_L^2 g_1\,\beta_{g_1} - 2g_{z'}Q_L^2\,\beta_{g_{z'}} \right) \\
m_{\tilde{\tau}^c}^2 &= \frac{m_{3/2}^2}{16\pi^2}\left(2y_\tau\,\beta_{y_\tau} - \frac{6}{5}Y_{e^c}^2 g_1\,\beta_{g_1} - 2g_{z'}Q_{e^c}^2\,\beta_{g_{z'}} \right) ;
\end{aligned}
\tag{4.3.7}
$$

and for the rest of the sleptons,

$$
\begin{aligned}
m_{\tilde{L}_i}^2 &= \frac{m_{3/2}^2}{16\pi^2}\left(-\frac{6}{4}g_2\,\beta_{g_2} - \frac{6}{5}Y_L^2 g_1\,\beta_{g_1} - 2g_{z'}Q_L^2\,\beta_{g_{z'}} \right) \\
m_{\tilde{e}_i^c}^2 &= \frac{m_{3/2}^2}{16\pi^2}\left(-\frac{6}{5}Y_{e^c}^2 g_1\,\beta_{g_1} - 2g_{z'}Q_{e^c}^2\,\beta_{g_{z'}} \right) \\
m_{\tilde{\nu}_i^c}^2 &= \frac{m_{3/2}^2}{16\pi^2}\left(-2g_{z'}Q_{\nu^c}^2\,\beta_{g_{z'}} \right) .
\end{aligned}
\tag{4.3.8}
$$

4.4 A terms

The non-zero Yukawa couplings are y_t, y_b, y_τ, λ, y_D and y_E. The corresponding A terms are:

$$A_t = -\beta_{y_t} m_{3/2}, \quad A_b = -\beta_{y_b} m_{3/2}, \quad A_\tau = -\beta_{y_\tau} m_{3/2},$$

$$A_\lambda = -\beta_\lambda m_{3/2}, \quad A_D = -\beta_{y_D} m_{3/2}, \quad A_E = -\beta_{y_E} m_{3/2}. \tag{4.4.1}$$

CHAPTER 5:   RGE EQUATIONS

To derive the RGEs we use the general expressions in [42, 43, 44].

5.1   Gauge and Yukawa couplings

The gauge coupling RGEs are

$$dg_i/d\ln\mu = \beta_{g_i}, \tag{5.1.1}$$

where $i = 1, 2, 3, Z'$ and the β_i are given in (4.1.1).

The Yukawa RGEs are

$$dy_i/d\ln\mu = \beta_{y_i}, \tag{5.1.2}$$

where $i = t, b, \tau, \lambda, D, E$ and the β_i are given in (4.1.2).

5.2 Gaugino masses

The RGEs for the gaugino masses are

$$
\frac{dM_1}{d\ln\mu} = \frac{g_1^2}{16\pi^2}\Bigg\{\frac{102}{5}M_1 + \frac{2}{16\pi^2}\Bigg[24g_3^2(M_1+M_3) + \frac{27}{5}g_2^2(M_1+M_2) + \frac{351}{25}g_1^2(2M_1)
$$

$$
+g_{z'}^2\frac{12}{5}\mathrm{Tr}\left(Y^2Q^2\right)(M_1+M_{\tilde Z'}))
$$

$$
+M_1\left(-\frac{26}{5}y_t^2 - \frac{14}{5}y_b^2 - \frac{18}{5}y_\tau^2 - \frac{6}{5}\lambda^2 - \frac{12}{5}y_D^2 - \frac{24}{5}y_E^2\right)
$$

$$
+\frac{26}{5}A_ty_t + \frac{14}{5}A_by_b + \frac{18}{5}A_\tau y_\tau + \frac{6}{5}A_\lambda\lambda + \frac{12}{5}A_Dy_D + \frac{24}{5}A_Ey_E\Bigg]\Bigg\}
$$

$$
\frac{dM_2}{d\ln\mu} = \frac{g_2^2}{16\pi^2}\Bigg\{2M_2 + \frac{2}{16\pi^2}\Bigg[24g_3^2(M_2+M_3) + 25g_2^2(2M_2) + \frac{9}{5}g_1^2(M_2+M_1)
$$

$$
+2g_{z'}^2(Q_{H_d}^2 + Q_{H_u}^2 + 3(Q_L^2 + 3Q_Q^2))(M_2+M_{\tilde Z'})
$$

$$
+M_2\left(-6y_t^2 - 6y_b^2 - 2y_\tau^2 - 2\lambda^2\right) + 6A_ty_t + 6A_by_b + 2A_\tau y_\tau + 2A_\lambda\lambda\Bigg]\Bigg\}
$$

$$
\frac{dM_3}{d\ln\mu} = \frac{2g_3^2}{(16\pi^2)^2}\Bigg[48g_3^2(2M_3) + 9g_2^2(M_3+M_2) + 3g_1^2(M_3+M_1) +
$$

$$
M_3\left(-4y_t^2 - 4y_b^2 - 6y_D^2\right) + 6g_{z'}^2(Q_D^2 + Q_{D^c}^2 + 2Q_Q^2 + Q_{u^c}^2 + Q_{d^c}^2)
$$

$$
(M_3+M_{\tilde Z'}) + 4A_ty_t + 4A_by_b + 6A_Dy_D\Bigg]
$$

$$
\frac{dM_{\tilde Z'}}{d\ln\mu} = \frac{g_{z'}^2}{16\pi^2}\Bigg\{2\mathrm{Tr}\left(Q^2\right)M_{\tilde Z'} + \frac{2}{16\pi^2}\Bigg[4g_{z'}^2\mathrm{Tr}\left(Q^4\right)(2M_{\tilde Z'}) +
$$

$$
g_1^2\frac{12}{5}\mathrm{Tr}\left(Y^2Q^2\right)(M_{\tilde Z'}+M_1) + 6g_2^2(Q_{H_d}^2 + Q_{H_u}^2 + 3(Q_L^2 + 3Q_Q^2))(M_{\tilde Z'}+M_2)
$$

$$
+48g_3^2(Q_D^2 + Q_{D^c}^2 + 2Q_Q^2 + Q_{u^c}^2 + Q_{d^c}^2)(M_{\tilde Z'}+M_3) + 12(Q_{u^c}^2 + Q_Q^2 + Q_{H_u}^2)
$$

$$
(A_t - M_{\tilde Z'}y_t)y_t + 12(Q_{d^c}^2 + Q_Q^2 + Q_{H_d}^2)(A_b - M_{\tilde Z'}y_b)y_b +
$$

$$
+4(Q_{H_d}^2 + Q_L^2 + Q_{e^c}^2)(A_\tau - M_{\tilde Z'}y_\tau) + 4(Q_{H_u}^2 + Q_{H_d}^2 + Q_S^2)(A_\lambda - M_{\tilde Z'}\lambda) +
$$

$$
+18(Q_{D^c}^2 + Q_D^2 + Q_S^2)(A_D - M_{\tilde Z'}y_D)y_D +
$$

$$
4(Q_{E^c}^2 + Q_E^2 + Q_S^2)(A_E - M_{\tilde Z'}y_E)y_E\lambda\Bigg]\Bigg\}.
$$

$$(5.2.1)$$

5.3 Scalar masses

The expression for RGEs of the soft masses, are for S, H_u, and H_d,

$$
\begin{aligned}
16\pi^2 \frac{dm_S^2}{d\ln\mu} &= -8g_{z'}^2 Q_S^2 M_{\tilde{Z}'}^2 + 4\lambda^2(m_S^2 + m_{H_u}^2 + m_{H_d}^2) \\
&\quad +6n_D y_D^2(m_S^2 + m_{\tilde{D}}^2 + m_{\tilde{D}^c}^2) + 2n_E y_E^2(m_S^2 + m_{\tilde{E}}^2 + m_{\tilde{E}^c}^2) \\
&\quad +4A_\lambda^2 + 2n_E A_E^2 + 6n_D A_D^2 \\
16\pi^2 \frac{dm_{H_u}^2}{d\ln\mu} &= -8g_{z'}^2 Q_{H_u}^2 M_{\tilde{Z}'}^2 - 6M_2^2 g_2^2 - \frac{24}{5} M_1^2 g_1^2 Y_{H_u}^2 \\
&\quad +2\lambda^2(m_S^2 + m_{H_u}^2 + m_{H_d}^2) + 6y_t^2(m_{H_u}^2 + m_{\tilde{Q}_3}^2 + m_{\tilde{t}^c}^2) + 6A_t^2 + 2A_\lambda^2 \\
16\pi^2 \frac{dm_{H_d}^2}{d\ln\mu} &= -8g_{z'}^2 Q_{H_d}^2 M_{\tilde{Z}'}^2 - 6M_2^2 g_2^2 - \frac{24}{5} M_1^2 g_1^2 Y_{H_d}^2 + 2\lambda^2(m_S^2 + m_{H_u}^2 + m_{H_d}^2) \\
&\quad +6y_b^2(m_{H_d}^2 + m_{\tilde{Q}_3}^2 + m_{\tilde{b}^c}^2) + 2y_\tau^2(m_{H_d}^2 + m_{\tilde{L}_3}^2 + m_{\tilde{\tau}^c}^2) \\
&\quad +6A_b^2 + 2A_\tau^2 + 2A_\lambda^2; \qquad (5.3.1)
\end{aligned}
$$

for the scalar exotics,

$$
\begin{aligned}
16\pi^2 \frac{dm_{\tilde{D}}^2}{d\ln\mu} &= -8g_{z'}^2 Q_D^2 M_{\tilde{Z}'}^2 - \frac{32}{3} M_3^2 g_3^2 - \frac{24}{5} M_1^2 g_1^2 Y_D^2 \\
&\quad +2y_D^2(m_S^2 + m_{\tilde{D}}^2 + m_{\tilde{D}^c}^2) + 2A_D^2 \\
16\pi^2 \frac{dm_{\tilde{D}^c}^2}{d\ln\mu} &= -8g_{z'}^2 Q_{D^c}^2 M_{\tilde{Z}'}^2 - \frac{32}{3} M_3^2 g_3^2 - \frac{24}{5} M_1^2 g_1^2 Y_{D^c}^2 + 2y_D^2(m_S^2 + m_{\tilde{D}}^2 + m_{\tilde{D}^c}^2) \\
&\quad +2A_D^2 \\
16\pi^2 \frac{dm_{\tilde{E}}^2}{d\ln\mu} &= -8g_{z'}^2 Q_E^2 M_{\tilde{Z}'}^2 - \frac{24}{5} M_1^2 g_1^2 Y_E^2 + 2y_E^2(m_S^2 + m_{\tilde{E}}^2 + m_{\tilde{E}^c}^2) + 2A_E^2 \\
16\pi^2 \frac{dm_{\tilde{E}^c}^2}{d\ln\mu} &= -8g_{z'}^2 Q_{E^c}^2 M_{\tilde{Z}'}^2 - \frac{24}{5} M_1^2 g_1^2 Y_{E^c}^2 + 2y_E^2(m_S^2 + m_{\tilde{E}}^2 + m_{\tilde{E}^c}^2) + 2A_E^2; \quad (5.3.2)
\end{aligned}
$$

for the third generation squarks,

$$16\pi^2 \frac{dm_{\tilde{Q}_3}^2}{d\ln\mu} = -8g_{z'}^2 Q_Q^2 M_{\tilde{Z}'}^2 - \frac{32}{3}M_3^2 g_3^2 - 6M_2^2 g_2^2 - \frac{24}{5}M_1^2 g_1^2 Y_Q^2$$
$$+2y_t^2(m_{H_u}^2 + m_{\tilde{Q}_3}^2 + m_{\tilde{t}^c}^2) + 2y_b^2(m_{H_d}^2 + m_{\tilde{Q}_3}^2 + m_{\tilde{b}^c}^2) + 2A_t^2 + 2A_b^2$$

$$16\pi^2 \frac{dm_{\tilde{t}^c}^2}{d\ln\mu} = -8g_{z'}^2 Q_{\tilde{u}^c}^2 M_{\tilde{Z}'}^2 - \frac{32}{3}M_3^2 g_3^2 - \frac{24}{5}M_1^2 g_1^2 Y_{u^c}^2 + 4y_t^2(m_{H_u}^2 + m_{\tilde{Q}_3}^2 + m_{\tilde{t}^c}^2) + 4A_t^2$$

$$16\pi^2 \frac{dm_{\tilde{b}^c}^2}{d\ln\mu} = -8g_{z'}^2 Q_{d^c}^2 M_{\tilde{Z}'}^2 - \frac{32}{3}M_3^2 g_3^2 - \frac{24}{5}M_1^2 g_1^2 Y_{d^c}^2 + 4y_b^2(m_{H_d}^2 + m_{\tilde{Q}_3}^2 + m_{\tilde{b}^c}^2) + 4A_b^2;$$

(5.3.3)

for the first two generations of squarks,

$$16\pi^2 \frac{dm_{\tilde{Q}_1}^2}{d\ln\mu} = -8g_{z'}^2 Q_Q^2 M_{\tilde{Z}'}^2 - \frac{32}{3}M_3^2 g_3^2 - 6M_2^2 g_2^2 - \frac{24}{5}M_1^2 g_1^2 Y_Q^2$$

$$16\pi^2 \frac{dm_{\tilde{u}_1^c}^2}{d\ln\mu} = -8g_{z'}^2 Q_{u^c}^2 M_{\tilde{Z}'}^2 - \frac{32}{3}M_3^2 g_3^2 - \frac{24}{5}M_1^2 g_1^2 Y_{u^c}^2$$

$$16\pi^2 \frac{dm_{\tilde{d}_1^c}^2}{d\ln\mu} = -8g_{z'}^2 Q_{d^c}^2 M_{\tilde{Z}'}^2 - \frac{32}{3}M_3^2 g_3^2 - \frac{24}{5}M_1^2 g_1^2 Y_{d^c}^2;$$

(5.3.4)

for the third generation of charged sleptons,

$$16\pi^2 \frac{dm_{\tilde{L}_3}^2}{d\ln\mu} = -8g_{z'}^2 Q_L^2 M_{\tilde{Z}'}^2 - 6M_2^2 g_2^2 - \frac{24}{5}M_1^2 g_1^2 Y_L^2 + 2y_\tau^2(m_{H_d}^2 + m_{\tilde{L}_3}^2 + m_{\tilde{\tau}^c}^2) + 2A_\tau^2$$

$$16\pi^2 \frac{dm_{\tilde{\tau}^c}^2}{d\ln\mu} = -8g_{z'}^2 Q_{e^c}^2 M_{\tilde{Z}'}^2 - \frac{24}{5}M_1^2 g_1^2 Y_{e^c}^2 + 4y_\tau^2(m_{H_d}^2 + m_{\tilde{L}_3}^2 + m_{\tilde{\tau}^c}^2) + 4A_\tau^2;$$

(5.3.5)

and for the rest of the sleptons,

$$16\pi^2 \frac{dm_{\tilde{L}}^2}{d\ln\mu} = -8g_{z'}^2 Q_L^2 M_{\tilde{Z}'}^2 - 6M_2^2 g_2^2 - \frac{24}{5}M_1^2 g_1^2 Y_L^2$$

$$16\pi^2 \frac{dm_{\tilde{e}^c}^2}{d\ln\mu} = -8g_{z'}^2 Q_{e^c}^2 M_{\tilde{Z}'}^2 - \frac{24}{5}M_1^2 g_1^2 Y_{e^c}^2$$

$$16\pi^2 \frac{dm_{\tilde{\nu}^c}^2}{d\ln\mu} = -8g_{z'}^2 Q_{\nu^c}^2 M_{\tilde{Z}'}^2.$$

(5.3.6)

5.4 A terms

The RGEs for the A terms are

$$
\begin{aligned}
16\pi^2 \frac{dA_t}{d\ln\mu} &= \frac{16}{3}g_3^2(2M_3 y_t - A_t) + 3g_2^2(2M_2 y_t - A_t) + \frac{13}{15}g_1^2(2M_1 y_t - A_t) \\
&\quad + 2g_{z'}^2(Q_{H_u}^2 + Q_Q^2 + Q_{u^c}^2)(2M_{\tilde{Z}'}y_t - A_t) \\
&\quad + 18A_t y_t^2 + y_b^2 A_t + 2A_b y_b\, y_t + \lambda^2 A_t + 2A_\lambda \lambda\, y_t \\
16\pi^2 \frac{dA_b}{d\ln\mu} &= \frac{16}{3}g_3^2(2M_3 y_b - A_b) + 3g_2^2(2M_2 y_b - A_b) + \frac{7}{15}g_1^2(2M_1 y_b - A_b) \\
&\quad + 2g_{z'}^2(Q_{H_d}^2 + Q_Q^2 + Q_{d^c}^2)(2M_{\tilde{Z}'}y_b - A_b) \\
&\quad + 18A_b y_b^2 + y_t^2 A_b + 2A_t y_t\, y_b + y_\tau^2 A_b + 2A_\tau y_\tau\, y_b + \lambda^2 A_b + 2A_\lambda \lambda\, y_b \\
16\pi^2 \frac{dA_\tau}{d\ln\mu} &= 3g_2^2(2M_2 y_\tau - A_\tau) + \frac{9}{5}g_1^2(2M_1 y_\tau - A_\tau) \\
&\quad + 2g_{z'}^2(Q_{H_d}^2 + Q_L^2 + Q_{e^c}^2)(2M_{\tilde{Z}'}y_\tau - A_\tau) \\
&\quad + 12A_\tau y_\tau^2 + 3y_b^2 A_\tau + 6A_b y_b\, y_\tau + \lambda^2 A_\tau + 2A_\lambda \lambda\, y_\tau \\
16\pi^2 \frac{dA_\lambda}{d\ln\mu} &= 3g_2^2(2M_2\lambda - A_\lambda) + \frac{3}{5}g_1^2(2M_1\lambda - A_\lambda) \\
&\quad + 2g_{z'}^2(Q_S^2 + Q_{H_u}^2 + Q_{H_d}^2)(2M_{\tilde{Z}'}\lambda - A_\lambda) \\
&\quad + A_\lambda(12\lambda^2 + 3y_t^2 + 3y_b^2 + y_\tau^2 + n_E y_E^2 + 3n_D y_D^2) \\
&\quad + \lambda(6y_t A_t + 6y_b A_b + 2y_\tau A_\tau + 2n_E y_E A_E + 6n_D y_D A_D) \\
16\pi^2 \frac{dA_{y_D}}{d\ln\mu} &= \frac{16}{3}g_3^2(2M_3 y_D - A_D) + \frac{6}{5}\left(Y_D^2 + Y_{D^c}^2\right)g_1^2(2M_1 y_D - A_D) \\
&\quad + 2g_{z'}^2(Q_S^2 + Q_D^2 + Q_{D^c}^2)(2M_{\tilde{Z}'}y_D - A_D) + A_D(2\lambda^2 + n_E y_E^2 +) \\
&\quad (9n_D + 6)y_D^2 + y_D(4\lambda A_\lambda + 2n_E y_E A_E) \\
16\pi^2 \frac{dA_{y_E}}{d\ln\mu} &= \frac{6}{5}\left(Y_E^2 + Y_{E^c}^2\right)g_1^2(2M_1 y_E - A_E) + 2g_{z'}^2(Q_S^2 + Q_E^2 + Q_{E^c}^2)(2M_{\tilde{Z}'}y_E - A_E) \\
&\quad + A_E(2\lambda^2 + 3n_D y_D^2 + (3n_E + 6)y_E^2) + y_E(4\lambda A_\lambda + 6n_D y_D A_D). \quad (5.4.1)
\end{aligned}
$$

CHAPTER 6:   SUMMARY

The results of this dissertation can be summarized as follows:

- The proton magnetic radius is extracted following the '*z-expansion*' method of Hill and Paz [7].

- Using proton scattering data, for a cut of $Q^2 \leq 0.5$ GeV^2, the radius is found to be $r_M^p = 0.91^{+0.03}_{-0.06} \pm 0.02$ fm.

- The value of the radius is $r_M^p = 0.87^{+0.04}_{-0.05} \pm 0.01$ fm by adding neutron data.

- $r_M^p = 0.87^{+0.02}_{-0.02}$ fm when the $\pi\pi$ data is added to the proton and neutron data.

- The neutron magnetic radius is also extracted to be $r_M^n = 0.89^{+0.03}_{-0.03}$ fm from the data sets combining proton, neutron, and $\pi\pi$.

- The most used formula in the literature for the Drell-Yan di-lepton production cross-section is found to be a factor of 8 small.

- Using the current LHC limit on stop mass, some parameter spaces are obtained which can be used for further analysis.

REFERENCES

[1] R. Frisch and O. Stern, Zeitschrift für Physik **85**, 4 (1933).

[2] J. R. Green, J. W. Negele, A. V. Pochinsky, S. N. Syritsyn, M. Engelhardt and S. Krieg, arXiv:1404.4029 [hep-lat].

[3] R. Pohl *et al.*, "The size of the proton," Nature **466**, 213 (2010).

[4] A. Antognini, F. Nez, K. Schuhmann, F. D. Amaro, FrancoisBiraben, J. M. R. Cardoso, D. S. Covita and A. Dax *et al.*, "Proton Structure from the Measurement of $2S - 2P$ Transition Frequencies of Muonic Hydrogen," Science **339**, 417 (2013).

[5] P. J. Mohr, B. N. Taylor and D. B. Newell, "CODATA Recommended Values of the Fundamental Physical Constants: 2010," arXiv:1203.5425 [physics.atom-ph].

[6] Z. Epstein, G. Paz and J. Roy, "Model independent extraction of the proton magnetic radius from electron scattering," arXiv:1407.5683 [hep-ph].

[7] R. J. Hill and G. Paz, "Model independent extraction of the proton charge radius from electron scattering," Phys. Rev. D **82**, 113005 (2010) doi:10.1103/PhysRevD.82.113005 arXiv:1008.4619 [hep-ph].

[8] J. Arrington, W. Melnitchouk and J. A. Tjon, "Global analysis of proton elastic form factor data with two-photon exchange corrections," arXiv:0707.1861 [nucl-ex].

[9] A. Lung, L. M. Stuart, P. E. Bosted, L. Andivahis, J. Alster, R. G. Arnold, C. C. Chang and F. S. Dietrich *et al.*, "Measurements of the electric and magnetic form-factors of the neutron from Q**2 = 1.75-GeV/c**2 to 4-GeV/c**2," Phys. Rev. Lett. **70**, 718 (1993).

[10] H. Gao, J. Arrington, E. J. Beise, B. Bray, R. W. Carr, B. W. Filippone, A. Lung and R. D. McKeown *et al.*, Phys. Rev. C **50**, 546 (1994).

[11] H. Anklin, D. Fritschi, J. Jourdan, M. Loppacher, G. Masson, I. Sick, E. E. W. Bruins and F. C. P. Joosse *et al.*, Phys. Lett. B **336**, 313 (1994).

[12] H. Anklin, L. J. deBever, K. I. Blomqvist, W. U. Boeglin, R. Bohm, M. Distler, R. Edelhoff and J. Friedrich *et al.*, Phys. Lett. B **428**, 248 (1998).

[13] G. Kubon, H. Anklin, P. Bartsch, D. Baumann, W. U. Boeglin, K. Bohinc, R. Bohm and M. O. Distler *et al.*, Phys. Lett. B **524**, 26 (2002) [nucl-ex/0107016].

[14] B. Anderson *et al.* [Jefferson Lab E95-001 Collaboration], Phys. Rev. C **75**, 034003 (2007) [nucl-ex/0605006].

[15] J. Lachniet *et al.* [CLAS Collaboration], Phys. Rev. Lett. **102**, 192001 (2009) [arXiv:0811.1716 [nucl-ex]].

[16] J. C. Bernauer *et al.* [A1 Collaboration], "High-precision determination of the electric and magnetic form factors of the proton," Phys. Rev. Lett. **105**, 242001 (2010) arXiv:1007.5076 [nucl-ex].

[17] D. Borisyuk, "Proton charge and magnetic rms radii from the elastic *ep* scattering data," arXiv:0911.4091 [hep-ph].

[18] M. A. Belushkin, H. W. Hammer and U. G. Meissner, "Dispersion analysis of the nucleon form factors including meson continua," arXiv:hep-ph/0608337.

[19] J. Beringer *et al.* [Particle Data Group Collaboration], "Review of Particle Physics (RPP)," Phys. Rev. D **86**, 010001 (2012).

[20] L. L. Foldy, "The Electromagnetic Properties of Dirac Particles," Phys. Rev. **87**, 688 (1952).

[21] G. Salzman, "Neutron-Electron Interaction," Phys. Rev. **99**, 973 (1955).

[22] F. J. Ernst, R. G. Sachs and K. C. Wali, "Electromagnetic form factors of the nucleon," Phys. Rev. **119**, 1105 (1960).

[23] P. Federbush, M. L. Goldberger and S. B. Treiman, Phys. Rev. **112**, 642 (1958).

[24] W. R. Frazer and J. R. Fulco, Phys. Rev. **117**, 1609 (1960).

[25] G. Höhler, Pion-nucleon scattering, in: H. Schopper (editor), Landolt-Börnstein database, Volume 9, subvolume b, part 1, Springer-Verlag, Berlin, 1983. [http://www.springermaterials.com/navigation/]

[26] P. Markowitz, J. M. Finn, B. D. Anderson, H. Arenhovel, A. R. Baldwin, D. Barkhuff, K. B. Beard and W. Bertozzi *et al.*, "Measurement of the magnetic form-factor of the neutron," Phys. Rev. C **48**, 5 (1993).

[27] E. E. W. Bruins, T. S. Bauer, H. W. den Bok, C. P. Duif, W. C. van Hoek, D. J. J. de Lange, A. Misiejuk and Z. Papandreou *et al.*, "Measurement of the neutron magnetic form-factor," Phys. Rev. Lett. **75**, 21 (1995).

[28] W. Xu, D. Dutta, F. Xiong, B. Anderson, L. Auberbach, T. Averett, W. Bertozzi and T. Black *et al.*, Phys. Rev. Lett. **85**, 2900 (2000) [nucl-ex/0008003].

[29] W. Xu *et al.* [Jefferson Lab E95-001 Collaboration], Phys. Rev. C **67**, 012201 (2003) [nucl-ex/0208007].

[30] http://clasweb.jlab.org/cgi-bin/clasdb/msm.cgi?eid=111&mid=1&data=on

[31] C. Patrignani *et al.* [Particle Data Group], "Review of Particle Physics," Chin. Phys. C **40**, no. 10, 100001 (2016). doi:10.1088/1674-1137/40/10/100001 PDG

[32] M. E. Peskin and D. V. Schroeder, "An Introduction to quantum field theory," Reading, USA: Addison-Wesley (1995).

[33] S. P. Martin, "A Supersymmetry primer," Adv. Ser. Direct. High Energy Phys. **21**, 1 (2010) arXiv:hep-ph/9709356.

[34] S. R. Coleman and J. Mandula, "All Possible Symmetries of the S Matrix," Phys. Rev. **159**, 1251 (1967). doi:10.1103/PhysRev.159.1251

[35] I. J. R. Aitchison, "Supersymmetry and the MSSM: An Elementary introduction," arXiv:hep-ph/0505105.

[36] M. A. Luty, "2004 TASI lectures on supersymmetry breaking," arXiv:hep-th/0509029.

[37] L. Randall and R. Sundrum, "Out of this world supersymmetry breaking," Nucl. Phys. B **557**, 79 (1999) doi:10.1016/S0550-3213(99)00359-4 hep-th/9810155.

[38] Z. Chacko, M. A. Luty, I. Maksymyk and E. Ponton, "Realistic anomaly mediated supersymmetry breaking," JHEP **0004**, 001 (2000) doi:10.1088/1126-6708/2000/04/001 hep-ph/9905390.

[39] P. Langacker, G. Paz, L. T. Wang and I. Yavin, "Z'-mediated Supersymmetry Breaking," Phys. Rev. Lett. **100**, 041802 (2008) arXiv:0710.1632 [hep-ph].

[40] P. Langacker, G. Paz, L. T. Wang and I. Yavin, "Aspects of Z-prime - mediated Supersymmetry Breaking," Phys. Rev. D **77**, 085033 (2008) doi:10.1103/PhysRevD.77.085033 arXiv:0801.3693 [hep-ph].

[41] J. de Blas, P. Langacker, G. Paz and L. T. Wang, "Combining Anomaly and Z-prime Mediation of Supersymmetry Breaking," JHEP **1001**, 037 (2010) doi:10.1007/JHEP01(2010)037 arXiv:0911.1996 [hep-ph].

[42] Y. Yamada, "Two loop renormalization of gaugino masses in general supersymmetric gauge models," Phys. Rev. Lett. **72**, 25 (1994) doi:10.1103/PhysRevLett.72.25 hep-ph/930830.

[43] S. P. Martin and M. T. Vaughn, "Two loop renormalization group equations for soft supersymmetry breaking couplings," Phys. Rev. D **50**, 2282 (1994) Erratum: [Phys. Rev. D **78**, 039903 (2008)] doi:10.1103/PhysRevD.50.2282, 10.1103/PhysRevD.78.039903 hep-ph/9311340

[44] Y. Yamada, "Two loop renormalization group equations for soft SUSY breaking scalar interactions: Supergraph method," Phys. Rev. D **50**, 3537 (1994) doi:10.1103/PhysRevD.50.3537 hep-ph/9401241

[45] D. Griffiths, Weinheim, Germany: Wiley-VCH (2008) 454 p

[46] V. Barger, P. Langacker, H. S. Lee and G. Shaughnessy, "Higgs Sector in Extensions of the MSSM," Phys. Rev. D **73**, 115010 (2006) doi:10.1103/PhysRevD.73.115010 hep-ph/0603247.

[47] G. Aad *et al.* [ATLAS Collaboration], "Observation of a new particle in the search for the Standard Model Higgs boson with the ATLAS detector at the LHC," Phys. Lett. B **716**, 1 (2012) doi:10.1016/j.physletb.2012.08.020 arXiv:1207.7214 [hep-ex].

[48] S. Chatrchyan *et al.* [CMS Collaboration], "Observation of a new boson at a mass of 125 GeV with the CMS experiment at the LHC," Phys. Lett. B **716**, 30 (2012) doi:10.1016/j.physletb.2012.08.021 arXiv:1207.7235 [hep-ex].

[49] P. Langacker, "The standard model and beyond" Boca Raton, USA: CRC Pr. (2010).

[50] E. Accomando, A. Belyaev, L. Fedeli, S. F. King and C. Shepherd-Themistocleous, "Z' physics with early LHC data," Phys. Rev. D **83**, 075012 (2011) doi:10.1103/PhysRevD.83.075012 arXiv:1010.6058 [hep-ph].

[51] F. Halzen and A. D. Martin, "Quarks And Leptons: An Introductory Course In Modern Particle Physics," New York, Usa: Wiley (1984)

[52] M. Carena, A. Daleo, B. A. Dobrescu and T. M. P. Tait, "Z' gauge bosons at the Tevatron," Phys. Rev. D **70**, 093009 (2004) doi:10.1103/PhysRevD.70.093009 arXiv:hep-ph/0408098.

[53] V. Khachatryan *et al.* [CMS Collaboration], "Search for physics beyond the standard model in dilepton mass spectra in proton-proton collisions at $\sqrt{s} = 8$ TeV," JHEP **1504**, 025 (2015) doi:10.1007/JHEP04(2015)025 arXiv:1412.6302 [hep-ex].

[54] P. Langacker, "The Physics of Heavy Z' Gauge Bosons," Rev. Mod. Phys. **81**, 1199 (2009) doi:10.1103/RevModPhys.81.1199 arXiv:0801.1345 [hep-ph].

[55] A. D. Martin, W. J. Stirling, R. S. Thorne and G. Watt, "Parton distributions for the LHC," Eur. Phys. J. C **63**, 189 (2009) doi:10.1140/epjc/s10052-009-1072-5 arXiv:0901.0002 [hep-ph].

[56] V. M. Abazov *et al.* [D0 Collaboration], "Search for a heavy neutral gauge boson in the dielectron channel with 5.4 fb-1 of $p\bar{p}$ collisions at sqrt(s) = 1.96 TeV," doi:10.1016/j.physletb.2010.10.059 arXiv:1008.2023 [hep-ex].

[57] The ATLAS collaboration [ATLAS Collaboration], "Search for a Scalar Partner of the Top Quark in the Jets+ETmiss Final State at $\sqrt{s} = 13$ TeV with the ATLAS detector," ATLAS-CONF-2017-020.

[58] T. Gherghetta, G. F. Giudice and J. D. Wells, "Phenomenological consequences of supersymmetry with anomaly induced masses," Nucl. Phys. B **559**, 27 (1999) doi:10.1016/S0550-3213(99)00429-0, arXiv:hep-ph/9904378.

[59] G. Paz and J. Roy, "Imposing LHC constraints on the combined Anomaly and Z' Mediation Mechanism of Supersymmetry Breaking"[*in preparation*].

ABSTRACT

TOPICS IN HIGH-ENERGY PHYSICS: THE PROTON MAGNETIC RADIUS AND PHENOMENOLOGY OF Z' MEDIATION OF SUPERSYMMETRY BREAKING

by

JOYDEEP ROY

December 2017

Advisor: Dr. Gil Paz
Major: Physics
Degree: Doctor of Philosophy

This dissertation describes two topics in high-energy physics. In the first we describe the extraction of the magnetic radius of the proton. In the second we impose LHC constraints on the combined anomaly and Z' mediation mechanisms of supersymmetry breaking.

We combine constraints from analyticity with experimental electron-proton scattering data to determine the proton magnetic radius without model-dependent assumptions on the shape of the form factor. We also study the impact of including electron-neutron scattering data, and $\pi\pi \to N\bar{N}$ data. Using representative data sets we find for a cut of $Q^2 \leq 0.5$ GeV^2, $r_M^p = 0.91^{+0.03}_{-0.06} \pm 0.02$ fm using just proton scattering data; $r_M^p = 0.87^{+0.04}_{-0.05} \pm 0.01$ fm adding neutron data; and $r_M^p = 0.87^{+0.02}_{-0.02}$ fm adding $\pi\pi$ data. We also extract the neutron magnetic radius from these data sets obtaining $r_M^n = 0.89^{+0.03}_{-0.03}$ fm from the combined proton, neutron, and $\pi\pi$ data. Particle Data Group (PDG) has reported both of these values, $r_M^p = 0.87 \pm 0.02$ fm and $r_M^n = 0.89 \pm 0.03$ fm in their 2016 listing of the magnetic radius of the proton and neutron, respectively.

Combining anomaly with Z' mediation allows us to solve the tachyonic problem of the former and avoid fine tuning in the latter. This model includes an extra $U(1)'$ gauge symmetry and extra singlet scalar S which provides a solution to the 'μ problem' of the MSSM. The low-energy particle spectrum is calculated from the UV inputs using

the Renormalization Group Equations. The benchmark points considered in the original model, suggested before the Higgs discovery, predicted a Higgs mass close to the current measured value of 125 GeV. We use the current LHC data to update the predictions of the model, its particle spectrum and in particular the mass of the Z' gauge boson.

AUTOBIOGRAPHICAL STATEMENT

EDUCATION

OCTOBER 2017   **Ph.D** in Theoretical Particle Physics,

Wayne State University, Detroit, U.S.A,

Advisor: Dr. GIL PAZ

DECEMBER 2014   **M.S** in Theoretical Particle Physics,

Wayne State University, Detroit, U.S.A,

Advisor: Dr. GIL PAZ

AUGUST 2009   **M.Sc** specialized in High Energy Physics,

Presidency University (College), Kolkata, INDIA

AUGUST 2007   **B.Sc** in Physics,

Presidency University (College), Kolkata, INDIA

PUBLICATIONS

1. Yu Gao, **J. Roy**, "*Probing leptoquark chirality via top polarization at the LHC*" (**Work in Progress**).

2. Gil Paz, **J. Roy**, "*Imposing LHC Constraints on the Combined Anomaly and Z'-Mediation Mechanism of Supersymmetry Breaking* (**Work in Progress**).

3. Gil Paz, **J. Roy**, "*A comment on the Z' Drell-Yan cross section*, arXiv:1711.02655 [hep-ph].

4. **J. Roy**, "*Imposing LHC Constraints on the combined Anomaly and Z'-Mediation Mechanism of Supersymmetry Breaking*, arXiv:1611.05004 [hep-ph].

5. Zachary Epstein, Gil Paz, and **J. Roy**, *Model independent analysis of the proton magnetic radius*, arXiv:1511.00664 [hep-ph].

6. Zachary Epstein, Gil Paz, and **J. Roy**, *Model independent extraction of the proton magnetic radius from electron scattering*, PhysRevD.90.074027, arXiv:1407.5683 [hep-ph].